

# Nuclear forces in the chiral limit

E. Epelbaum,<sup>†#1</sup> Ulf-G. Meißner,<sup>‡#2</sup> W. Glöckle<sup>†#3</sup>

<sup>†</sup>*Ruhr-Universität Bochum, Institut für Theoretische Physik II,  
D-44870 Bochum, Germany*

<sup>‡</sup>*Forschungszentrum Jülich, Institut für Kernphysik (Theorie),  
D-52425 Jülich, Germany*

and

*Karl-Franzens-Universität Graz, Institut für Theoretische Physik  
A-8010 Graz, Austria*

## Abstract

We investigate the behaviour of the nuclear forces as a function of the light quark masses (or, equivalently, pion mass) in the framework of chiral effective field theory at next-to-leading order. The nucleon–nucleon force is described in terms of one and two–pion exchange and local short distance operators, which depend explicitly and implicitly on the quark masses. The pion propagator becomes Coulomb-like in the chiral limit and thus one has significant scattering in all partial waves. The pion-nucleon coupling depends implicitly on the quark masses and we find that it becomes stronger in the chiral limit. There is a further quark mass dependence in the S-wave four–nucleon couplings, which can be estimated by means of dimensional analysis. We find that nuclear physics in the chiral limit becomes natural. There are no new bound states, the deuteron binding energy is  $B_D^{\text{CL}} = 9.6 \pm 1.9^{+1.8}_{-1.0}$  MeV, and the S-wave scattering lengths take values of a few fm,  $a_{\text{CL}}(^1S_0) = -4.1 \pm 1.6^{+0.0}_{-0.4}$  fm and  $a_{\text{CL}}(^3S_1) = 1.5 \pm 0.4^{+0.2}_{-0.3}$  fm. We also discuss the extrapolation to larger pion masses pertinent for the extraction of these quantities from lattice simulations.

---

<sup>#1</sup>email: [evgeni.epelbaum@tp2.ruhr-uni-bochum.de](mailto:evgeni.epelbaum@tp2.ruhr-uni-bochum.de)

<sup>#2</sup>email: [u.meissner@fz-juelich.de](mailto:u.meissner@fz-juelich.de)

<sup>#3</sup>email: [walter.gloeckle@tp2.ruhr-uni-bochum.de](mailto:walter.gloeckle@tp2.ruhr-uni-bochum.de)

# 1 Introduction

The application of (chiral) effective field theory (EFT) to few-nucleon systems has become a subject of vigorous research interest in the last years. One successful method is based upon the original idea of Weinberg [1] to apply the standard methods of Chiral Perturbation Theory (CHPT) to the kernel of the corresponding integral equation (Lippmann–Schwinger equation in case of two nucleons and Faddeev–Yakubovsky equations for three and more nucleons), and consequently solving it numerically. The necessity of summing the interactions to an infinite order is caused by the nonperturbative aspects of the problem (shallow nuclear bound states, unnaturally large S-wave scattering lengths), quite in contrast to the purely perturbative treatment possible in the pion and pion–nucleon sectors. The complete analysis of two- and three-nucleon systems and, in addition, of the  $\alpha$ -particle has been recently performed up to next-to-next-to-leading order (NNLO) in the chiral expansion [2, 3, 4, 5]. Going to NNLO turns out to be sufficient to describe accurately most of the low-energy observables. CHPT is an effective field theory based upon the approximate and spontaneously broken chiral symmetry of QCD and allows for a model-independent and systematic way of calculating low-energy hadronic observables. This is achieved by a simultaneous expansion in small external momenta and quark (pion) masses around the chiral limit, in which the light quarks (and, as a consequence, also Goldstone bosons) are massless. Since this expansion is well defined for sufficiently small quark masses ( $m_q$ ), hadronic properties at low energies are expected not to change strongly in the limit  $m_q \rightarrow 0$ . This feature is of crucial importance for the applicability of CHPT and is certainly valid in the purely pionic sector. In the chiral limit the interaction between pions becomes arbitrarily weak for vanishing external momenta. The complete one-loop analysis for the two flavor case has been performed by Gasser and Leutwyler in 1984 [6]. By now, the two-loop analysis of the  $\pi\pi$  scattering and other selected S-matrix elements and transition currents has become available, see e.g. [7]. In the pion–nucleon case the situation is similar, since the coupling of the Goldstone bosons to matter fields vanishes at small momentum transfer in the chiral limit as well. The loop expansion in the presence of the additional mass scale (i.e. the nucleon mass in the chiral limit) is somewhat more tricky, but various methods have been invented to allow for a consistent and symmetry preserving power counting. The purpose of the present work is to consider the nucleon–nucleon (NN) interaction in the chiral limit. Clearly, this case requires additional care because of the nonperturbative aspects of the problem and also due to the fact that the interaction between nucleons does not become weak in the chiral limit.<sup>#4</sup> In principle, at very low energies one may consider a theory of nucleons only interacting via contact interactions, the so-called pionless EFT (see e.g. [8] and references therein). While such a scheme has been shown to be a precise calculational tool, the link to the chiral symmetry is lost and we thus eschew such type of EFT here.<sup>#5</sup> We stress that the question about the  $M_\pi$ -dependence of nuclear forces is not only of academic interest, but also of practical use since such studies of quark mass dependences can be used to interpolate lattice gauge theory data, which are usually obtained for quark (pion) masses much larger than physical ones. Furthermore, the deuteron and other light nuclei can be considered as laboratories to test the recent ideas of the time variation of certain fundamental couplings constants (see e.g. [9] and references therein).

The first step in extrapolating the properties of the NN system for vanishing quark mass (exact chiral symmetry of QCD) was done by Bulgac et al. [10] a few years ago. They stressed that the vanishing pion mass may potentially lead to strong effects in the nucleon–nucleon P- and higher partial waves. One could even not exclude a priori the presence of bound states in some of the P-waves in the chiral limit. This indicates that in case of few-nucleon systems, the expansion around the chiral limit might be complicated or even not well defined. Based upon the one-pion exchange potential (OPEP) and

---

<sup>#4</sup>Moreover, it even gets stronger in most channels, as we will show below.

<sup>#5</sup>In the pionless EFT the pion mass is considered to be a large scale and the limit  $M_\pi \rightarrow 0$  cannot be performed.

taking into account only its explicit dependence on the pion mass, the authors of ref. [10] came to the conclusion that no bound states appear in P- and higher partial waves in the chiral limit. Performing first-order perturbation theory and using the deuteron wave-functions from some phenomenological potential models, Bulgac et al. found a reduction of about 1 MeV (that is by 50%) in the deuteron binding energy. The main conclusion of ref. [10] was therefore that "... physics of nuclei in a universe where  $M_\pi = 0$  would be similar to what is actually observed." However, the interpretation of the results found in [10] requires some caution not only due to the fact that first-order perturbative results can not be trusted in that case,<sup>#6</sup> but also because only the explicit dependence on the pion mass has been taken into account. In the language of chiral effective field theory, taking into account only the explicit  $M_\pi$ -dependence in the OPEP corresponds (roughly) to the LO approximation, which is not accurate enough to lead to any quantitative conclusions.

More recently, Beane et al. re-analyzed the situation in the  $^1S_0$  and  $^3S_1 - ^3D_1$  channels including also some implicit dependence of the NN interaction on the pion mass [11]. They considered the OPEP as an approximation to the NN interaction for distances larger than some matching radius  $R_\star$ . For shorter distances the potential was approximated by a square well, which can be viewed as a smeared out delta-function counter term. In the  $^3S_1 - ^3D_1$ -channel they also included an additional energy-dependent contribution in the short-range part of the potential. Adjusting the two parameters related to the short range part of the interaction, Beane et al. performed exact renormalization of the corresponding Schrödinger equation, i.e. the calculated low-energy observables do not depend on the matching radius  $R_\star$ . This way of handling the diverging Schrödinger equation is closely related to their previous work [12]. The situation in the chiral limit has been analyzed in two ways: (i) Keeping only the explicit  $M_\pi$  dependence of the OPEP an increase of the deuteron binding energy by about a factor of two has been found,  $B_d \sim 4.2$  MeV. (ii) The authors of ref.[11] also made an attempt to take into account the implicit  $M_\pi$ -dependence, which changes the strength of the OPEP in the chiral limit. They further assumed that these corrections can be represented by the leading logarithmic terms in the chiral expansion.<sup>#7</sup> Quite surprisingly, the results for deuteron binding energy were found to change completely after taking into account the implicit  $M_\pi$ -dependence in this manner. It turned out that deuteron becomes unbound for the pion mass smaller than  $\sim 100$  MeV. Another interesting issue discussed in [11] refers to the possibility of matching the results obtained in chiral effective field theory with the ones from lattice QCD [13], which requires extrapolation away from the physical value of  $M_\pi$ .

While this paper was in preparation, an NLO analysis of the quark mass dependence in the  $^1S_0$  and  $^3S_1 - ^3D_1$  channels by Beane and Savage based upon the power counting introduced in ref. [11] has become available [14], improving and extending the results of ref. [11]. Apart from the OPE and short-range terms in the effective potential, the leading TPE contribution (in the chiral limit) has been taken into account. The authors found evidence for nearly all possible scenarios such as a bound or unbound deuteron and di-neutron in the  $^1S_0$  channel and could not make any predictions for the corresponding scattering lengths due to the lack of knowledge of the low-energy constants related to contact terms with one insertion proportional to  $M_\pi^2$ . We will come back to this work and to comparison to our results in the next-to-last section.

The aim of this work is to perform a complete NLO calculation in the framework of a modified Weinberg power counting and to try to clarify the presently somewhat controversial situation about the chiral limit of the nucleon-nucleon interaction <sup>#8</sup>. To do that, we have to consider apart from the

---

<sup>#6</sup>As pointed out in [11], one gets a deuteron binding energy  $B_d \sim 4.1$  MeV if the pion mass is set to zero in the AV18 potential. Thus the effect is of the opposite sign to the one found in [10] using first-order perturbation theory.

<sup>#7</sup>Note that this assumption goes beyond standard CHPT and is not applicable in a general case. We will come back to this point later on.

<sup>#8</sup>This is similar to what was done in [14] but differs markedly in some aspects from that work as will be shown below.

OPEP and contact interactions also the leading two-pion exchange potential (TPEP). We will discuss in detail the renormalization of the NN potential at NLO since this is of utmost importance for such type of analysis. We will not use of the assumption of the dominance of chiral logarithms but rather work with the complete CHPT expressions at this order. The corresponding low-energy constants (LECs) will be taken from the analysis of various processes. We will demonstrate that using only the leading logarithms leads to results for the renormalization of the axial coupling  $g_A$  incompatible with the present analyses of the  $\pi N$  system and of the process  $\pi N \rightarrow \pi\pi N$ . We also perform an extrapolation of the  $^1S_0$  and  $^3S_1$  scattering lengths and deuteron binding energy  $B_D$  for the values of the pion mass in the range  $0 < M_\pi < 300$  MeV.

Our manuscript is organized as follows. In section 2 we consider the chiral effective nucleon-nucleon potential at next-to-leading order, with particular emphasis on the aspects of renormalization pertinent to derive the desired quark mass dependences. Such an analysis is not yet available in the literature. We also demonstrate the equivalence between the S-matrix approach used to analyze the pion-nucleon sector and the non-covariant projection formalism employed to construct the NN potential. We systematically work out all explicit and implicit quark mass dependences of the various contributions due to one- and two-pion exchanges as well as contact interactions. Results for the NN phase shifts, the deuteron binding energy and the S-wave scattering lengths are collected in section 3. Will also discuss in detail the differences to the earlier EFT work [11, 14]. A brief summary and further discussion is presented in section 4.

## 2 Nucleon–nucleon potential at next–to–leading order

In this section, we remind the reader on the structure of the NN potential at NLO and perform its complete renormalization, which is of crucial importance for considering the chiral limit. This has not been done in our previous work [3], since we were only interested in constructing the potential for the physically relevant case. Since different methods have been applied in the literature to define the effective interaction it appears necessary to begin our considerations with a brief overview of some commonly used formalisms. This topic is also of technical importance because the pion-exchange is directly linked to the pion-nucleon sector, and thus consistency with the field theoretical NN potential has to be demonstrated. The reader more interested in the explicit form of the potential at NLO exhibiting explicit and implicit pion mass dependences may directly proceed to section 2.4.

### 2.1 Construction of the NN potential from field theory

The construction of a potential from field theory is a well known and intensively studied problem in nuclear physics. Historically, the important conceptual achievements in that direction have been done in the fifties in the context of the so called meson field theory. The problem can be formulated in the following way: given some field theoretical Lagrangian for interacting mesons and nucleons, how can one reduce the (infinite dimensional) equation of motion for mesons and nucleons to an effective Schrödinger equation for nucleonic degrees of freedom, which can then be solved by standard methods? It goes beyond the scope of this paper to discuss the whole variety of the different techniques which have been developed to construct an effective interactions, see ref. [15] for a comprehensive review. We will now briefly introduce two methods which will be important for our further considerations. The first method is closely related to the field theoretical S-matrix given (in the interaction representation) by

$$S_{\alpha\beta} = \delta_{\alpha\beta} - 2\pi i \delta(E_\alpha - E_\beta) T_{\alpha\beta}, \quad (2.1)$$

where the T-matrix  $T_{\alpha\beta}$  satisfies:

$$T_{\alpha\beta} = V_{\alpha\beta} + V_{\alpha\gamma}(E_\beta - E_\gamma + i\epsilon)^{-1}T_{\gamma\beta}. \quad (2.2)$$

Inverting the last equation one obtains the following equation for the effective potential  $V_{\alpha\beta}$ :

$$V_{\alpha\beta} = T_{\alpha\beta} - T_{\alpha\gamma}(E_\beta - E_\gamma + i\epsilon)^{-1}T_{\gamma\beta} + \dots, \quad (2.3)$$

where the ellipsis refer to higher order iterations in the T-matrix. The effective potential  $V_{\alpha\beta}$  can now be obtained in terms of a perturbative expansion for the T-matrix. For example, in the Yukawa theory one can calculate  $T_{\alpha\beta}$  (and also  $V_{\alpha\beta}$ ) in terms of a power series expansion in the squared meson-nucleon coupling constant  $g^2$ . It has to be pointed out that the potential  $V_{\alpha\beta}$  in eq. (2.3) is not defined unambiguously since only on the energy shell T-matrix elements are known and well-defined in field theory. In fact, at any fixed order of the perturbative expansion (2.3) one can perform an arbitrary off-the-energy shell extension of the potential, which will then affect even on the energy shell matrix elements at higher orders. In addition, one has a freedom to perform field redefinitions, which changes off shell S-matrix elements and, as a consequence, off shell matrix elements of the potential. Such an ambiguity of the effective potential is a general property and does not pose any problem, since the latter is not observable. Only observable quantities, i.e. on shell S-matrix elements, binding energies, ..., are defined unambiguously in quantum field theory.

The method introduced above has been used by Kaiser et al. to derive the NN potential from the chiral Lagrangian [16, 17] and will be referred to in what follows as the S-matrix method. Its close relation to the scattering amplitude makes it possible to apply the standard field theoretical techniques for calculation the effective interactions.

Another well known scheme is often referred to as the Tamm-Dancoff method [18, 19]. The starting point is the time-independent Schrödinger equation

$$(H_0 + H_I)|\Psi\rangle = E|\Psi\rangle, \quad (2.4)$$

where  $|\Psi\rangle$  denotes an eigenstate of the Hamiltonian  $H$  with the eigenvalue  $E$ . One can now divide the full Fock space into the nucleonic subspace  $|\phi\rangle$  and the complementary one  $|\psi\rangle$  and rewrite the Schrödinger equation (2.4) as

$$\begin{pmatrix} \eta H \eta & \eta H \lambda \\ \lambda H \eta & \lambda H \lambda \end{pmatrix} \begin{pmatrix} |\phi\rangle \\ |\psi\rangle \end{pmatrix} = E \begin{pmatrix} |\phi\rangle \\ |\psi\rangle \end{pmatrix}, \quad (2.5)$$

where we introduced the projection operators  $\eta$  and  $\lambda$  such that  $|\phi\rangle = \eta|\Psi\rangle$ ,  $|\psi\rangle = \lambda|\Psi\rangle$ . Expressing the state  $|\psi\rangle$  from the second line of the matrix equation (2.5) as

$$|\psi\rangle = \frac{1}{E - \lambda H \lambda} H |\phi\rangle, \quad (2.6)$$

and substituting this into the first line we obtain the Schrödinger-like equation for the projected state  $|\phi\rangle$ :

$$(H_0 + V_{\text{eff}}(E)) |\phi\rangle = E |\phi\rangle, \quad (2.7)$$

with an effective potential  $V_{\text{eff}}(E)$  given by

$$V_{\text{eff}}(E) = \eta H_I \eta + \eta H_I \lambda \frac{1}{E - \lambda H \lambda} \lambda H_I \eta. \quad (2.8)$$

Eq. (2.7) differs from the ordinary Schrödinger equation by the fact that the effective potential  $V_{\text{eff}}(E)$  depends explicitly on the energy, as it is obvious from the definition (2.8). In fact, such an explicit

energy dependence can be eliminated from the potential as discussed e.g. in ref.[21]. Indeed, the effective potential  $V_{\text{eff}}(E)$  up to the fourth order in the coupling constant  $g$  in the Yukawa theory with  $H_I = gH^1$  is given in a symbolic form as

$$(V_{\text{eff}}(E))_{mn} = g^2 \frac{H_{m\alpha}^1 H_{\alpha n}^1}{E - E_\alpha} + g^4 \frac{H_{m\alpha}^1 H_{\alpha\beta}^1 H_{\beta\gamma}^1 H_{\gamma n}^1}{(E - E_\alpha)(E - E_\beta)(E - E_\gamma)} + \mathcal{O}(g^6). \quad (2.9)$$

We denote here the states from the  $\eta$ -subspace by latin letters and the ones from the  $\lambda$ -subspace by greek letters. Using the relation

$$(E - E_n)\langle n|\phi\rangle = \mathcal{O}(g^2)\langle n|\phi\rangle, \quad (2.10)$$

we can substitute  $E$  in the denominator of the last term in eq. (2.9) by  $E_n$ . Thus we can now express eq. (2.7) in the form:

$$\left( g^2 \frac{H_{m\alpha}^1 H_{\alpha n}^1}{E - E_\alpha} + g^4 \frac{H_{m\alpha}^1 H_{\alpha\beta}^1 H_{\beta\gamma}^1 H_{\gamma n}^1}{(E - E_\alpha)(E - E_\beta)(E - E_\gamma)} \right) \langle n|\phi\rangle + \mathcal{O}(g^6) = (E - E_m) \langle m|\phi\rangle. \quad (2.11)$$

The first term in the left-hand side of this equation can be expressed in the form

$$g^2 \frac{H_{m\alpha}^1 H_{\alpha n}^1}{E - E_\alpha} \langle n|\phi\rangle = \left( g^2 \frac{H_{m\alpha}^1 H_{\alpha n}^1}{E_n - E_\alpha} + g^2 \frac{H_{m\alpha}^1 H_{\alpha n}^1}{(E - E_\alpha)(E_n - E_\alpha)} (E_n - E) \right) \langle n|\phi\rangle. \quad (2.12)$$

Performing an iteration of eq. (2.11) one expresses the last term in the right-hand side of eq. (2.12) as a fourth order term and replace  $E$  by  $E_n$ . The final result for the energy independent Tamm-Dancoff potential, which differs from the original one in eq. (2.8) by higher order terms, is then

$$(V_{\text{eff}})_{mn} = g^2 \frac{H_{m\alpha}^1 H_{\alpha n}^1}{E_n - E_\alpha} + g^4 \frac{H_{m\alpha}^1 H_{\alpha\beta}^1 H_{\beta\gamma}^1 H_{\gamma n}^1}{(E_n - E_\alpha)(E_n - E_\beta)(E_n - E_\gamma)} - g^4 \frac{H_{m\alpha}^1 H_{\alpha l}^1 H_{l\gamma}^1 H_{\gamma n}^1}{(E_n - E_\alpha)(E_l - E_\alpha)(E_n - E_\gamma)}. \quad (2.13)$$

Even after elimination of the explicit energy dependence, eq. (2.7) does not correspond to the ordinary Schrödinger equation since the resulting effective Hamiltonian turns out to be non-hermitean. The problem is that the projected nucleon states  $|\phi\rangle$  have a normalization different from the the states  $|\Psi\rangle$  we have started from, which are assumed to span a complete and orthonormal set in the whole Fock space:

$$\langle \phi_i | \phi_j \rangle = \langle \Psi_i | \Psi_j \rangle - \langle \psi_i | \psi_j \rangle = \delta_{ij} - \langle \phi_i | H_I \lambda \left( \frac{1}{E - \lambda H \Lambda} \right)^2 \lambda H_I \phi_j \rangle. \quad (2.14)$$

Note that the components  $\psi_i$  in this equation do, in general, not vanish. Thus in order to end up with the ordinary Schrödinger equation one has to switch from the set  $\{\phi\}$  of eigenstates of eq. (2.7) which is assumed to be complete in the  $\eta$ -subspace<sup>#9</sup> but is not orthonormal, to another complete **and orthonormal** set  $\{\chi\}$ . This has been achieved in an elegant way by Fukuda et al. [20] and Okubo [21]. They introduced an operator  $A \equiv \lambda A \eta$  which maps the states  $\phi$  into the states  $\psi$ :

$$|\psi\rangle = A|\phi\rangle, \quad (2.15)$$

so that the state  $\Psi$  is given by

$$|\Psi\rangle = (1 + A)|\phi\rangle. \quad (2.16)$$

<sup>#9</sup>This is presumably true at least in the case of weakly interacting fields.

The operator  $A$  is equivalent to the operator which enters eq. (2.6) with the only difference of being energy independent. One can show that it has to satisfy the equation [21]:

$$\lambda (H - [A, H] - AHA) \eta = 0 . \quad (2.17)$$

It is now obvious that the states  $|\chi\rangle$

$$|\chi\rangle = (1 + A^\dagger A)^{1/2} |\phi\rangle \quad (2.18)$$

lie in the  $\eta$ -subspace and are normalized properly. The effective Schrödinger equation for  $|\chi\rangle$  can now be derived from eqs. (2.5), (2.15), (2.17) and (2.18), see ref. [21]:

$$(H_0 + \tilde{V}_{\text{eff}}) |\chi\rangle = E |\chi\rangle, \quad (2.19)$$

with the effective potential given by

$$\tilde{V}_{\text{eff}} = (1 + A^\dagger A)^{-1/2} (\eta + A^\dagger) H (\eta + A) (1 + A^\dagger A)^{-1/2} - H_0 . \quad (2.20)$$

A more elegant way to end up with the same effective Schrödinger equation has been proposed by Okubo by using a unitary transformation of the form

$$U = \begin{pmatrix} \eta(1 + \tilde{A}^\dagger \tilde{A})^{-1/2} & -\tilde{A}^\dagger(1 + \tilde{A}\tilde{A}^\dagger)^{-1/2} \\ \tilde{A}(1 + \tilde{A}^\dagger \tilde{A})^{-1/2} & \lambda(1 + \tilde{A}\tilde{A}^\dagger)^{-1/2} \end{pmatrix}, \quad (2.21)$$

with the operator  $\tilde{A} = \lambda \tilde{A} \eta$ . The operator  $\tilde{A}$  has to satisfy the decoupling equation (2.17) in order for the transformed Hamiltonian to be of block-diagonal form and can (under certain circumstances) be identified with the operator  $A$  from eq. (2.15). In [2] we have shown how to solve the decoupling equation (2.17) and to derive the nuclear force according eq. (2.20) using the methods of CHPT. In what follows we will perform a complete renormalization of the NN potential at NLO and demonstrate that the renormalized expressions for the potential in this formalism (with the specific choice of the unitary operator given in eq. (2.21)) agrees with the one obtained by using the S-matrix methods. We will also show how to perform renormalization in the method of unitary transformation and how to include pion tadpole contributions and recover the same expressions for renormalized quantities as found in covariant perturbation theory using the technique of Feynman diagrams. It is important to perform a complete renormalization of the effective Hamiltonian and to take into account all the implicit dependence on the quark (or, equivalently pion) mass.

Before closing this section we would like to stress that the effective Hamiltonian derived with the method of unitary transformation is by no means a unique one, as it has also been the case in the S-matrix method. The unitary operator (2.21) is not the most general one. Indeed, it is always possible to perform additional unitary transformations in  $\eta$  and  $\lambda$ -subspaces, which are not taken into account in the definition (2.21). The above unitary transformation is in that sense the “minimal” one. This ambiguity with respect to the effective Hamiltonian clearly does not mean that the physically observed quantities are defined ambiguously. In what follows, will not be concerned any more with these subtleties.

## 2.2 One-pion exchange contribution to the scattering amplitude

The contribution from the OPE to the NN force shown in fig. 1 appears (in Weinberg’s power counting) at leading order (LO) in the chiral expansion together with two different contact interactions without derivatives. The OPEP gets renormalized at NLO due to pion loops and counter term insertions. As

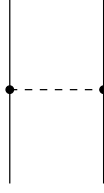


Figure 1: Leading order one-pion exchange. The solid (dashed) lines refer to nucleons (pions). The heavy dots are leading order vertices from  $\mathcal{L}_{\pi N}^{(1)}$ . The diagrams resulting from interchange of the nucleon lines are not shown.

discussed in the previous section, the renormalized OPEP in the S-matrix method is defined by off-the-energy shell extension of the field-theoretical amplitude. The corresponding diagrams are shown in fig. 2. The graphs 1–4 lead to the renormalization of the nucleon lines, while the diagrams 10 and 11 contribute to renormalization of the pion line and 7–9 renormalize the pion–nucleon coupling. The contribution from graphs 5 and 6 involves an odd power of the loop momentum  $l$  to be integrated over and thus vanishes. The underlying chiral Lagrangians are given by:

$$\begin{aligned}
\mathcal{L}_{\pi\pi}^{(2)} &= \frac{F^2}{4} \langle \nabla^\mu U \nabla_\mu U^\dagger + \chi_+ \rangle, \\
\mathcal{L}_{\pi\pi}^{(4)} &= \frac{l_3}{16} \langle \chi_+ \rangle^2 \\
&\quad + \frac{l_4}{16} \left\{ 2 \langle \nabla_\mu U \nabla^\mu U^\dagger \rangle \langle \chi_+ \rangle + 2 \langle \chi^\dagger U \chi^\dagger U + \chi U^\dagger \chi U^\dagger \rangle - 4 \langle \chi^\dagger \chi \rangle - \langle \chi_+ \rangle^2 \right\} + \dots, \\
\mathcal{L}_{\pi N}^{(1)} &= \bar{N}_v \left[ i(v \cdot D) + \overset{\circ}{g}_A (S \cdot u) \right] N_v, \\
\mathcal{L}_{\pi N}^{(2)} &= \bar{N}_v \left[ \frac{1}{2 \overset{\circ}{m}} (v \cdot D)^2 - \frac{1}{2 \overset{\circ}{m}} D \cdot D + c_1 \langle \chi_+ \rangle \right] N_v + \dots, \\
\mathcal{L}_{\pi N}^{(3)} &= \bar{N}_v \left[ d_{16} S \cdot u \langle \chi_+ \rangle + i d_{18} S^\mu [D_\mu, \chi_-] + \tilde{d}_{28} (i \langle \chi_+ \rangle v \cdot D + \text{h.c.}) \right] N_v + \dots,
\end{aligned} \tag{2.22}$$

where  $F$ ,  $\overset{\circ}{g}_A$  and  $\overset{\circ}{m}$  refer to the bare pion decay constant, the bare nucleon axial vector coupling constant and the bare nucleon mass<sup>#10</sup> and  $c_1$  and  $d_i$  are low-energy constants. The brackets  $\langle \rangle$  denote traces in the flavor space. We adopted here the heavy baryon formulation for nucleon fields, with  $v_\mu$  and  $S_\mu = (1/2)i\gamma_5\sigma_{\mu\nu}v^\nu$  denoting the four-velocity and spin operator, respectively. The unitary  $2 \times 2$  matrix  $U$  in the flavor space collects the pion fields and is defined in the  $\sigma$ -model gauge, which we will use throughout this work, as:

$$U = \frac{1}{F} \left[ \sqrt{F^2 - \pi^2} + i\boldsymbol{\tau} \cdot \boldsymbol{\pi} \right]. \tag{2.23}$$

Further,

$$\begin{aligned}
u &= \sqrt{U}, & u_\mu &= i(u^\dagger \partial_\mu u - u \partial_\mu u^\dagger), & D_\mu &= \partial_\mu + \Gamma_\mu, \\
\Gamma_\mu &= \frac{1}{2} [u^\dagger, \partial_\mu u], & \chi_\pm &= u^\dagger \chi u^\dagger \pm u \chi^\dagger u, & \chi &= 2B(s + ip),
\end{aligned} \tag{2.24}$$

<sup>#10</sup>If dimensional regularization is used,  $F$ ,  $\overset{\circ}{g}_A$  and  $\overset{\circ}{m}$  coincide with the corresponding constants in the chiral limit.



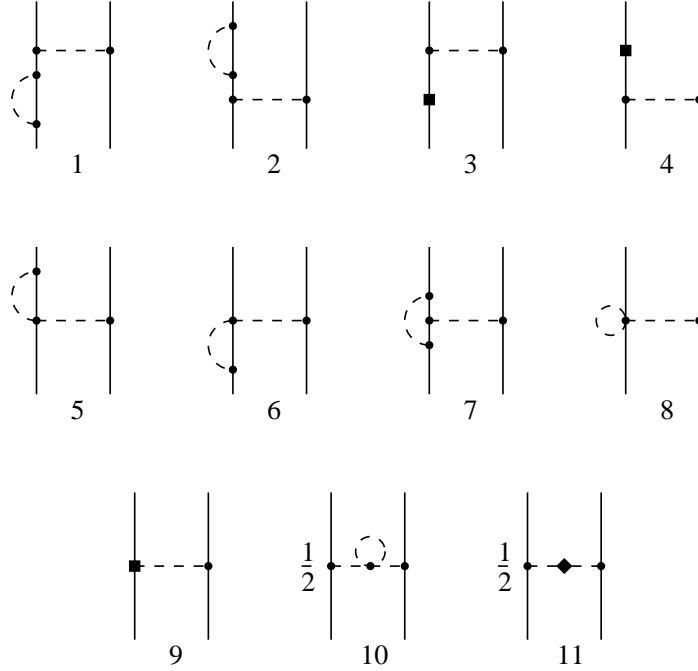


Figure 2: Diagrams contributing to the renormalization of the OPE. The heavy dots are leading order vertices from  $\mathcal{L}_{\pi N}^{(1)}$  and  $\mathcal{L}_{\pi\pi}^{(2)}$  while the solid rectangles correspond to vertices from  $\mathcal{L}_{\pi N}^{(3)}$  (in case of diagrams 3 and 4 also from  $\mathcal{L}_{\pi N}^{(2)}$ ). The solid diamond represents insertions from  $\mathcal{L}_{\pi\pi}^{(4)}$ . For remaining notation see fig. 1.

where the quantity  $B$  is just a constant. We do not take into account external vector and axial-vector fields. The physically relevant values for scalar and pseudoscalar sources  $s$  and  $p$  are

$$s(x) = \mathcal{M}, \quad p(x) = 0, \quad (2.25)$$

where  $\mathcal{M}$  denotes the quark mass matrix. Note that we have only shown explicitly the terms in eq. (2.22) we will use in our calculation. We also note that  $1/\overset{\circ}{m}$  terms are suppressed in Weinberg's approach and would appear one order higher. Further details on construction and structure of the effective Lagrangian can be found in [22, 23, 24, 25, 26].

The OPE at leading order corresponds to the diagram shown in fig. 1 and is given by

$$\mathcal{A}_{\text{OPE}} = \frac{\overset{\circ}{g}_A^2}{F^2} (\boldsymbol{\tau}_1 \cdot \boldsymbol{\tau}_2) \frac{1}{q^2 - M^2} (S_1 \cdot q)(S_2 \cdot q). \quad (2.26)$$

Here  $q$  denotes the momentum transfer of the nucleon, i.e.  $q = p' - p$ , where  $p'$  and  $p$  are final and initial nucleon momenta. Further,  $M$  is the leading term in the quark mass expansion of the pion mass. The more convenient expression in the rest-frame system of the nucleons<sup>#11</sup> with  $v_\mu = (1, 0, 0, 0)$  and

<sup>#11</sup>We are only interested in the specific kinematic, in which both nucleons move with the same velocity  $v_\mu$  and the relative momentum is small.

$S^\mu = (0, 1/2 \vec{\sigma})$ , where the  $\sigma_i$  are the Pauli spin matrices reads

$$\mathcal{A}_{\text{OPE}}^{\text{NC}} = -\frac{\overset{\circ}{g}_A^2}{(2F)^2} \frac{1}{\vec{q}^2 + M^2} (\vec{\sigma}_1 \cdot \vec{q}) (\vec{\sigma}_2 \cdot \vec{q}) + \mathcal{O}(m^{-2}). \quad (2.27)$$

We have introduced here the superscript NC (= “noncovariant”) in order to distinguish between the noncovariant notation of eq. (2.27) and covariant one in eq. (2.26). The noncovariant notation is appropriate for calculation of the S–matrix based upon the effective Hamilton operator. Note that the physical values  $g_A$ ,  $F_\pi$  and  $M_\pi$  of the axial nucleon coupling, pion decay coupling and pion mass can be used in the expression for the OPE if one restricts oneself to the LO analysis.

We will now evaluate the NLO corrections to the OPE, which result from the diagrams shown in fig. 2. The calculation can easily be performed using e.g. the Feynman rules from [22, 25]. The diagrams 1,...,4 renormalize external the nucleon lines and lead to

$$\mathcal{A}_{1,2,3,4} = ((Z_N)^2 - 1) \mathcal{A}_{\text{OPE}}. \quad (2.28)$$

Here  $Z_N$  is the nucleon Z–factor given by

$$Z_N = 1 + \Sigma'(0). \quad (2.29)$$

The nucleon self–energy  $\Sigma(\tilde{\omega})$  ( $\tilde{\omega} = v \cdot k$ ,  $k$ –nucleon momentum) is given up to order  $Q^2$  ( $Q$  refers to a generic small momentum scale) by

$$\Sigma(\tilde{\omega}) = -4M^2 \left( c_1 + 2\tilde{d}_{28}\tilde{\omega} \right) + 3i \frac{\overset{\circ}{g}_A^2}{F^2} \int \frac{d^4l}{(2\pi)^4} \frac{i}{v \cdot (k-l) + i\epsilon} \frac{i}{l^2 - M^2 + i\epsilon} (S \cdot l)(-S \cdot l). \quad (2.30)$$

We will now proceed in two ways. First, we apply dimensional regularization and the same subtraction as in ref. [24] and recover the standard results for the amplitude. Secondly, in order to compare our results with the ones obtained in the method of unitary transformation we will go into the rest–frame system with  $v_\mu = (1, 0, 0, 0)$  and  $S^\mu = (0, 1/2 \vec{\sigma})$ , where the  $\sigma_i$  are the Pauli spin matrices and perform integrations over zeroth component of the loop momentum  $l$  via contour methods. Furthermore, we will not restrict ourselves to any specific regularization scheme in that case since we are only interested in the general structure of the amplitude. The divergent integrals are always to be understood as being regularized by some standard methods. In order to distinguish the results obtained in this way from the ones found using dimensional regularization and the subtraction defined in ref. [24] we will denote the latter ones by the superscript DR.

For the nucleon Z–factor  $Z_N$  in eq. (2.29) we find:

$$\begin{aligned} Z_N^{\text{DR}} &= 1 - \frac{3 \overset{\circ}{g}_A^2 M^2}{32\pi^2 F^2} \left[ 3 \ln \frac{M}{\lambda} + 1 \right] - 8M^2 \tilde{d}_{28}^r(\lambda), \\ Z_N &= 1 - 3 \frac{\overset{\circ}{g}_A^2}{8F^2} J_{13} - 8M^2 \tilde{d}_{28}. \end{aligned} \quad (2.31)$$

where we have introduced

$$J_{mn} = \int \frac{d^3l}{(2\pi)^3} \frac{l^{2m}}{\omega_l^n}. \quad (2.32)$$

Clearly,  $Z_N^{\text{DR}}$  can also be obtained directly from  $Z_N$  performing dimensional regularization in three dimensions of the divergent integral  $J_{13}$ .

The nucleon mass shift is related to the self energy via

$$m_N = \overset{\circ}{m} + \delta m_N, \quad \delta m_N = \Sigma(0). \quad (2.33)$$

Using dimensional regularization one finds

$$\delta m_N^{\text{DR}} = -4c_1 M^2 - \frac{3 \overset{\circ}{g}_A^2 M^3}{32\pi F^2}, \quad (2.34)$$

while the unregularized expression (after performing integration over the zeroth component  $l_0$  of the loop momentum) reads:

$$\delta m_N = -4c_1 M^2 - \frac{3 \overset{\circ}{g}_A^2}{8F^2} J_{12}. \quad (2.35)$$

Notice that the mass of the nucleon does not appear explicitly in the expressions for the NN potential at NLO but enters the two-nucleon propagator in the Lippmann–Schwinger equation. We will discuss this issue later on.

For diagrams 7,8,9 in fig. 2 we obtain in dimensional regularization (D.R.)

$$\begin{aligned} \mathcal{A}_{7,8,9}^{\text{DR}} &= Z_{7,8,9}^{\text{DR}} \mathcal{A}_{\text{OPE}}, \\ Z_{7,8,9}^{\text{DR}} &= \frac{2M^2 L(\lambda)}{F^2} + \frac{M^2}{16\pi^2 F^2} \left[ (\overset{\circ}{g}_A^2 + 2) \ln \frac{M}{\lambda} + \overset{\circ}{g}_A^2 \right] + \frac{8M^2 d_{16}^r(\lambda)}{\overset{\circ}{g}_A} - \frac{4M^2 d_{18}}{\overset{\circ}{g}_A}, \end{aligned} \quad (2.36)$$

where we used the same definitions for  $L(\lambda)$  and  $d_{16}^r(\lambda)$  as in [24]. Note that the constant  $d_{18}$ , which leads to the Goldberger–Treiman discrepancy, is finite and does not get renormalized. Switching to the noncovariant notation and performing integration over  $l_0$  we find the following unregularized expressions for these quantities:

$$\begin{aligned} \mathcal{A}_{7,8,9} &= Z_{7,8,9} \mathcal{A}_{\text{OPE}}^{\text{NC}}, \\ Z_{7,8,9} &= -\frac{\overset{\circ}{g}_A^2}{4F^2} \left( 1 - d + \frac{2}{d-1} \right) J_{13} + \frac{1}{2F^2} J_{01} + \frac{8M^2 d_{16}}{\overset{\circ}{g}_A} - \frac{4M^2 d_{18}}{\overset{\circ}{g}_A}, \end{aligned} \quad (2.37)$$

where  $d = 4$  in the physically relevant case of (3+1) space-time dimensions.

Finally, renormalization of the pion line in graphs 10 and 11 in fig. 2 leads to

$$\mathcal{A}_{10,11} = \left( \delta Z_\pi + \frac{\delta M^2}{q^2 - M^2} \right) \mathcal{A}_{\text{OPE}}, \quad (2.38)$$

where

$$\begin{aligned} Z_\pi &= 1 + \delta Z_\pi, \quad \delta Z_\pi = -\frac{\Delta_\pi}{F^2} - \frac{2M^2}{F^2} l_4, \\ M_\pi^2 &= M^2 + \delta M_\pi^2, \quad \delta M_\pi^2 = M^2 \left\{ \frac{\Delta_\pi}{2F^2} + \frac{2M^2}{F^2} l_3 \right\}, \end{aligned} \quad (2.39)$$

Here,  $M_\pi$  is the physical value of the pion mass. The last term in the brackets in eq. (2.38) gives the correction to the one-pion exchange due to the shift in the pion mass and should be ignored if the physical value of the pion mass is used in the expression (2.26) for the OPE at LO. The quantity  $\Delta_\pi$  is given in D.R. by

$$\Delta_\pi^{\text{DR}} = 2M^2 \left( L(\lambda) + \frac{1}{16\pi^2} \ln \frac{M}{\lambda} \right) + \mathcal{O}(d-4), \quad (2.40)$$

and in the previously introduced notation with divergent integrals  $J_{ij}$  just by  $\Delta_\pi = 1/2 J_{01}$ . Note that in the calculation of the pion wave function renormalization and mass shift one has to take into account the noncovariant pion propagator of the form:

$$\delta_{ab}\Delta_{\mu\nu}(k) = \int d^4x \langle 0|T\partial_\mu\pi_a(x)\partial_\nu\pi_b(0)|0\rangle = \frac{ik_\mu k_\nu}{k^2 - M^2 + i\eta} - ig_{\mu 0}g_{\nu 0}, \quad (2.41)$$

as discussed in [29]. Such noncovariant pieces in the pion propagators (as well as noncovariant pieces in the interaction Hamiltonian arising from time derivatives) are usually omitted if one works in dimensional regularization. This does not lead to wrong results since the missing terms correspond to power-law divergences, which vanish in D.R.. However, in a general case such noncovariant pieces should be taken into account. For instance, if the last piece in the above expression is omitted and cut-off regularization is used, pions become massive in the chiral limit due to the tadpole diagram. Summing up the contributions of all graphs in fig. 2 we obtain the renormalized OPE as

$$\mathcal{A}_{\text{OPE}}^{\text{ren}} = -\frac{1}{4} \left( \frac{g_A}{F_\pi} \right)^2 \left( 1 - \frac{4M_\pi^2 d_{18}}{g_A} \right) \frac{\boldsymbol{\tau}_1 \cdot \boldsymbol{\tau}_2}{\vec{q}^2 + M_\pi^2} (\vec{\sigma} \cdot \vec{q}) (\vec{\sigma} \cdot \vec{q}), \quad (2.42)$$

where  $g_A/F_\pi$  is given in D.R. by

$$\frac{g_A}{F_\pi} = \frac{\overset{\circ}{g}_A}{F} \left( 1 - \frac{g_A^2 M_\pi^2}{4\pi^2 F_\pi^2} \ln \frac{M_\pi}{\lambda} - \frac{g_A^2 M_\pi^2}{16\pi^2 F_\pi^2} - 8M_\pi^2 \tilde{d}_{28}^r(\lambda) + \frac{4M_\pi^2}{g_A} d_{16}^r(\lambda) - \frac{M_\pi^2}{F_\pi^2} l_4^r(\lambda) \right) \quad (2.43)$$

Note that we substituted  $\overset{\circ}{g}_A$  and  $F_\pi$  in the brackets in the right-hand side of above equations by their renormalized values  $g_A$  and  $F_\pi$ , which is correct at this order. If one is only interested in the real world observables, which correspond to the physical value of the pion mass, one can equally well rewrite this expression in terms of scale independent LECs  $\bar{d}_{16}$  and  $\bar{l}_4$  as follows:

$$\frac{g_A}{F_\pi} = \frac{\overset{\circ}{g}_A}{F} \left( 1 - \frac{g_A^2 M_\pi^2}{16\pi^2 F_\pi^2} + \frac{4M_\pi^2}{g_A} \bar{d}_{16} - \frac{M_\pi^2}{16\pi^2 F_\pi^2} \bar{l}_4 \right). \quad (2.44)$$

The LECs  $\bar{d}_{16}$  and  $\bar{l}_4$  are defined according to refs. [24] and [6]:

$$\begin{aligned} d_{16}^r(\lambda) &\equiv d_{16} - \frac{\kappa_{16}}{F^2} L(\lambda) = \bar{d}_{16} - \frac{\kappa_{16}}{(4\pi F)^2} \ln \frac{\lambda}{M}, \\ l_4^r(\lambda) &\equiv l_4 - 2L(\lambda) = \frac{1}{16\pi^2} \bar{l}_4 + \frac{1}{8\pi^2} \ln \frac{M}{\lambda}, \end{aligned} \quad (2.45)$$

where  $\kappa_{16} = \overset{\circ}{g}_A (4 - \overset{\circ}{g}_A^2)/8$ . The renormalized LEC  $\tilde{d}_{28}$  has no finite piece (or, in other words, the corresponding scale-independent LEC  $\tilde{\tilde{d}}_{28}$  vanishes):

$$\tilde{d}_{28}^r(\lambda) \equiv \tilde{d}_{28} - \frac{\tilde{\kappa}_{28}}{F^2} L(\lambda) = -\frac{\tilde{\kappa}_{28}}{(4\pi F)^2} \ln \frac{\lambda}{M}, \quad (2.46)$$

with  $\tilde{\kappa}_{28} = -9/16 \overset{\circ}{g}_A^2$ . Thus the corresponding counter term in the first line of eq. (2.31) cancels against the logarithmic term. We note that it is a convention that the contact terms needed for renormalization do not have a finite part. In principle, one could allow for such contributions but that would only lead to a reshuffling of the finite parts of other LECs. If one insists on working with the minimal number of independent terms, such a choice has to be taken (as discussed in more detail in [24]).

Finally, we display the unregularized expression for the ratio  $g_A/F_\pi$ :

$$\frac{g_A}{F_\pi} = \frac{\overset{\circ}{g}_A}{F} \left( 1 - \frac{g_A^2}{8F_\pi^2} \left( 4 - d + \frac{2}{d-1} \right) J_{13} - \frac{M_\pi^2}{F_\pi^2} l_4 - 8M_\pi^2 \tilde{d}_{28} + \frac{4M_\pi^2}{g_A} d_{16} \right). \quad (2.47)$$

### 2.3 One–pion exchange from the method of unitary transformations

Let us now calculate the renormalized OPEP using the method of unitary transformation, following the lines of refs. [2, 3]. The essential difference compared to our previous work [2] is that we now have to take into account pion tadpole contributions. The corresponding diagrams lead to renormalization of various parameters in the effective Lagrangian and were of no importance in the previous calculations [3], where physical values for renormalized coupling constants have been used. The pion tadpole contributions are, however, important for the present analysis, since they lead to an additional pion mass dependence of various renormalized quantities. In the following we will show how to deal with the pion tadpoles and how to perform complete and consistent renormalization in the method of unitary transformation. We would also like to stress that renormalization of the effective Hamilton operator within the method of unitary transformation has been considered recently in a different context, see refs. [27, 28].

Let us begin with the effective Lagrangian  $\mathcal{L}_{\pi\pi}$  for pions given in the first two lines of eq. (2.22). The relevant terms in the  $\sigma$ -model gauge, eq. (2.23), read:

$$\begin{aligned}\mathcal{L}_{\pi\pi}^{(2)} &= \frac{1}{2} (\partial_\mu \boldsymbol{\pi} \cdot \partial^\mu \boldsymbol{\pi} - M^2 \boldsymbol{\pi}^2) + \frac{1}{2F^2} (\partial_\mu \boldsymbol{\pi} \cdot \boldsymbol{\pi})^2 - \frac{1}{8F^2} M^2 \boldsymbol{\pi}^4 + \dots \\ \mathcal{L}_{\pi\pi}^{(4)} &= -\frac{l_3 M^4}{F^2} \boldsymbol{\pi}^2 + \frac{l_4 M^2}{F^2} \partial_\mu \boldsymbol{\pi} \cdot \partial^\mu \boldsymbol{\pi} - \frac{l_4 M^4}{F^2} \boldsymbol{\pi}^2 + \dots\end{aligned}\quad (2.48)$$

We now introduce the renormalized pion field and mass:

$$\begin{aligned}\boldsymbol{\pi}_r &= Z_\pi^{-1/2} \boldsymbol{\pi}, & Z_\pi &= 1 + \delta Z_\pi, \\ M_\pi^2 &= M^2 + \delta M_\pi^2,\end{aligned}\quad (2.49)$$

where  $\delta Z_\pi$ ,  $(\delta M_\pi^2)/M_\pi^2 \sim \mathcal{O}(Q^2/\Lambda_\chi^2)$ . We express eq. (2.48) in terms of the renormalized pion field and mass by simply replacing  $\boldsymbol{\pi} \rightarrow \boldsymbol{\pi}_r$ ,  $M^2 \rightarrow M_\pi^2$  and  $\mathcal{L}_{\pi\pi}^{(4)} \rightarrow \mathcal{L}_{\pi\pi}^{(4)} + \delta(\mathcal{L}_{\pi\pi}^{(4)})$  where

$$\delta(\mathcal{L}_{\pi\pi}^{(4)}) = \frac{1}{2} \delta Z_\pi \partial_\mu \boldsymbol{\pi}_r \cdot \partial^\mu \boldsymbol{\pi}_r - \frac{1}{2} M_\pi^2 \left( \delta Z_\pi - \frac{\delta M_\pi^2}{M_\pi^2} \right) \boldsymbol{\pi}_r^2 + \dots\quad (2.50)$$

Here the ellipses refer to terms with more pion fields. In what follows we will always work with renormalized pion fields and therefore omit the subscript  $r$ .

The Hamilton density corresponding to the Lagrangian introduced above can be derived using the canonical formalism and following the lines of [29]. Let us first express the effective Lagrangian in a more compact form:

$$\mathcal{L}_{\pi\pi} = \frac{1}{2} \partial_\mu \pi_a G_{ab}(\boldsymbol{\pi}) \partial^\mu \pi_b - \frac{M_\pi^2}{2} \boldsymbol{\pi}^2 B(\boldsymbol{\pi}),\quad (2.51)$$

where

$$\begin{aligned}G_{ab}(\boldsymbol{\pi}) &= \delta_{ab} \left( 1 + \delta Z_\pi + \frac{2l_4 M_\pi^2}{F^2} \right) + \frac{1}{F^2} \pi_a \pi_b + \dots = \delta_{ab} + \tilde{G}_{ab}(\boldsymbol{\pi}), \\ B(\boldsymbol{\pi}) &= 1 + \delta Z_\pi - \frac{\delta M_\pi^2}{M_\pi^2} + \frac{2l_3 M_\pi^2}{F^2} + \frac{2l_4 M_\pi^2}{F^2} + \frac{1}{4F^2} \boldsymbol{\pi}^2 + \dots = 1 + \tilde{B}(\boldsymbol{\pi}).\end{aligned}\quad (2.52)$$

Here the subscripts  $a, b$  correspond to isospin indices. For the momentum  $\Pi_a$  conjugate to the field  $\pi_a$  we get:

$$\Pi_a = \frac{\delta \mathcal{L}_{\pi\pi}}{\delta \partial_0 \pi_a} = G_{ab}(\boldsymbol{\pi}) \partial_0 \pi_b.\quad (2.53)$$

The Hamiltonian  $\mathcal{H}_{\pi\pi}$  is given by

$$\mathcal{H}_{\pi\pi} = \Pi_a G_{ab}^{-1}(\boldsymbol{\pi}) \Pi_b - \mathcal{L}_{\pi\pi} = \frac{1}{2} \Pi_a G_{ab}^{-1}(\boldsymbol{\pi}) \Pi_b - \frac{1}{2} \partial_i \pi_a G_{ab}(\boldsymbol{\pi}) \partial^i \pi_b + \frac{M_\pi^2}{2} \boldsymbol{\pi}^2 B(\boldsymbol{\pi}). \quad (2.54)$$

We now divide the Hamiltonian into its free and interaction part as follows:

$$\begin{aligned} \mathcal{H}_{\pi\pi} &= \mathcal{H}_{\pi\pi}^0 + \mathcal{H}_{\pi\pi}^I, \\ \mathcal{H}_{\pi\pi}^0 &= \frac{1}{2} \Pi_a \Pi_a - \frac{1}{2} \partial^i \pi_a \partial_i \pi_a + \frac{M_\pi^2}{2} \boldsymbol{\pi}^2, \\ \mathcal{H}_{\pi\pi}^I &= -\frac{1}{2} \partial_\mu \pi_a \tilde{G}_{ab}(\boldsymbol{\pi}) \partial^\mu \pi_b - \frac{1}{2} \partial_0 \pi_a \tilde{G}_{ab}^2(\boldsymbol{\pi}) \partial_0 \pi_b + \frac{1}{2} M_\pi^2 \boldsymbol{\pi}^2 \tilde{B}(\boldsymbol{\pi}). \end{aligned} \quad (2.55)$$

Since the field operators  $\pi_a$ ,  $\partial_i \pi_a$  and  $\Pi_a$  transform simply into the interaction picture (IP),  $\pi_a \rightarrow \pi_a^{\text{IP}}$ ,  $\partial_i \pi_a \rightarrow (\partial_i \pi_a)^{\text{IP}}$  and  $\Pi_a \rightarrow (\partial_0 \pi_a)^{\text{IP}}$ , we can easily express the interaction Hamiltonian  $\mathcal{H}_{\pi\pi}^I$  in the IP representation as:<sup>#12</sup>

$$\begin{aligned} \mathcal{H}_{\pi\pi}^I &= -\frac{1}{2} \partial_\mu \pi_a \tilde{G}_{ab}(\boldsymbol{\pi}) \partial^\mu \pi_b + \frac{1}{2} M_\pi^2 \boldsymbol{\pi}^2 \tilde{B}(\boldsymbol{\pi}) + \frac{1}{2} \partial_0 \pi_a \left\{ \tilde{G}^2(\boldsymbol{\pi}) (1 + \tilde{G}(\boldsymbol{\pi}))^{-1} \right\}_{ab} \partial_0 \pi_b \\ &= -\frac{1}{2} \partial_\mu \boldsymbol{\pi} \cdot \partial^\mu \boldsymbol{\pi} \left( \delta Z_\pi + \frac{2l_4 M_\pi^2}{F^2} \right) + \frac{1}{2} M_\pi^2 \boldsymbol{\pi}^2 \left( \delta Z_\pi - \frac{\delta M_\pi^2}{M_\pi^2} + \frac{2l_3 M_\pi^2}{F^2} + \frac{2l_4 M_\pi^2}{F^2} \right) \\ &\quad - \frac{1}{2F^2} (\boldsymbol{\pi} \cdot \partial_\mu \boldsymbol{\pi}) (\boldsymbol{\pi} \cdot \partial^\mu \boldsymbol{\pi}) + \frac{1}{8F^2} M_\pi^2 \boldsymbol{\pi}^4 + \dots, \end{aligned} \quad (2.56)$$

where we have omitted the superscripts IP. We now write  $\pi_a(x)$  in terms of creation and annihilation operators  $a_a^\dagger(\vec{k})$ ,  $a_a(\vec{k})$  as

$$\pi_a(x) = \int \frac{d^3 k}{(2\pi)^{3/2}} \frac{1}{\sqrt{2\omega_k}} \left[ e^{-ik \cdot x} a_a(\vec{k}) + e^{ik \cdot x} a_a^\dagger(\vec{k}) \right], \quad (2.57)$$

where  $\omega_k = \sqrt{\vec{k}^2 + M_\pi^2}$  and the operators  $a_a(\vec{k})$  and  $a_a^\dagger(\vec{k})$  satisfy the commutation relations

$$\left[ a_a(\vec{k}), a_b(\vec{k}') \right] = \left[ a_a^\dagger(\vec{k}), a_b^\dagger(\vec{k}') \right] = 0, \quad \left[ a_a(\vec{k}), a_b^\dagger(\vec{k}') \right] = \delta_{ab} \delta(\vec{k} - \vec{k}'). \quad (2.58)$$

Substituting eq. (2.57) into eq. (2.56) and performing normal ordering, we end up with terms of the form  $a^\dagger a$ ,  $a^\dagger a^\dagger$ ,  $aa$ ,  $a^\dagger a^\dagger aa$ ,  $\dots$ . In fig. 3 we show symbolically the contributions to the Hamiltonian of the form  $a^\dagger a$ ,  $a^\dagger a^\dagger$  and  $aa$ . Note that the closed loops result from contraction of the operators  $a$  and  $a^\dagger$  in the terms in the last line of eq. (2.56) when bringing these into normal ordered form. For example, for the term of the form  $a^\dagger a$  we get the following expression:

$$\begin{aligned} H_{\pi\pi}^I &= \sum_a \int d^3 k \frac{1}{\omega_k} a_a^\dagger(\vec{k}) a_a(\vec{k}) \left\{ \frac{1}{2} k^2 \left( -\delta Z_\pi - \frac{2l_4 M_\pi^2}{F^2} - \frac{1}{2F^2} J_{01} \right) \right. \\ &\quad \left. + \frac{1}{2} M_\pi^2 \left( \delta Z_\pi - \frac{\delta M_\pi^2}{M_\pi^2} + \frac{2l_3 M_\pi^2}{F^2} + \frac{2l_4 M_\pi^2}{F^2} + \frac{3}{4F^2} J_{01} \right) \right\} + \dots \end{aligned} \quad (2.59)$$

We now require that there are no terms of the form  $a^\dagger a$ ,  $a^\dagger a^\dagger$  and  $aa$  in the interaction Hamiltonian at the order considered in the chiral expansion (since we already work with the renormalized pion fields). Then we obtain from eqs. (2.49), (2.59):

$$\begin{aligned} Z_\pi &= 1 - \frac{2l_4 M_\pi^2}{F^2} - \frac{1}{2F^2} J_{01}, \\ M_\pi^2 &= M^2 \left( 1 + \frac{2l_3 M_\pi^2}{F^2} + \frac{1}{4F^2} J_{01} \right). \end{aligned} \quad (2.60)$$

<sup>#12</sup>In the last line of eq. (2.55) one has first to replace  $\partial_0 \pi_a$  by  $G_{ab}^{-1}(\boldsymbol{\pi}) \Pi_b$ .

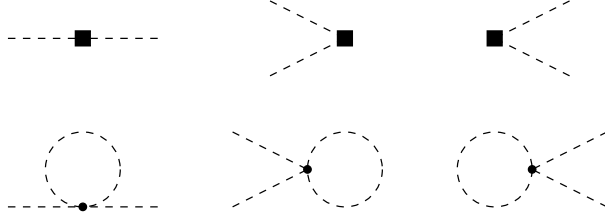


Figure 3: Contributions to the one-pion Hamiltonian. The heavy dots are leading order vertices from  $\mathcal{L}_{\pi\pi}^{(2)}$  while the solid rectangles correspond to vertices from  $\mathcal{L}_{\pi\pi}^{(4)} + \delta(\mathcal{L}_{\pi\pi}^{(4)})$ .

These expressions coincide precisely with the ones found using the S-matrix method, eq. (2.39). Let us now include nucleons. The relevant terms in the effective Lagrangian  $\mathcal{L}_{\pi N}$  from eq. (2.22) are

$$\begin{aligned}
\mathcal{L}_{\pi N}^{(1)} &= N^\dagger \left( i\partial_0 - \frac{\overset{\circ}{g}_A}{2F} \boldsymbol{\tau} \boldsymbol{\sigma} \cdot \vec{\nabla} \boldsymbol{\pi} - \frac{\overset{\circ}{g}_A}{4F^3} (\boldsymbol{\pi} \boldsymbol{\sigma} \cdot \vec{\nabla} \boldsymbol{\pi}) \boldsymbol{\tau} \cdot \boldsymbol{\pi} \right) N + \dots, \\
\mathcal{L}_{\pi N}^{(2)} &= N^\dagger \left( \delta m_N + \frac{\vec{\nabla}^2}{2m_N} + 4c_1 M_\pi^2 \right) N + \dots, \\
\mathcal{L}_{\pi N}^{(3)} &= N^\dagger \left( \left( -\frac{2M_\pi^2 d_{16}}{F} + \frac{M_\pi^2 d_{18}}{F} - \frac{\overset{\circ}{g}_A}{4F} \delta Z_\pi \right) \boldsymbol{\tau} \boldsymbol{\sigma} \cdot \vec{\nabla} \boldsymbol{\pi} + 8i\tilde{d}_{28} M_\pi^2 \partial_0 \right) N + \dots.
\end{aligned} \tag{2.61}$$

Here several comments are in order. First, the superscript ( $i$ ) in the above Lagrangians refers, as in eq. (2.22), just to the number of derivatives and/or pion mass insertion. Secondly, we prefer to use the physical and not the bare mass of the nucleon in the heavy baryon expansion, i.e. we parameterize the four-momentum of the nucleon  $p_\mu$  as  $p_\mu = m_N v_\mu + l_\mu$ , where  $l_\mu$  is a small residual momentum  $v \cdot l \ll m_N$ . Expressing the Lagrangian in terms of the physical instead of the bare nucleon mass is, of course, just a matter of convenience and all results remain unchanged. The physical and bare nucleon masses are related by

$$m_N = \overset{\circ}{m} + \delta m_N, \quad \delta m_N = \delta m_N^{(2)} + \delta m_N^{(3)} + \dots, \quad \delta m_N^{(i)} \sim \mathcal{O}(Q^i). \tag{2.62}$$

Note that  $\delta m_N^{(2)} = -4c_1 M_\pi^2$  as can be seen from the second line of eq. (2.61).<sup>#13</sup> As in the previous section we restrict ourselves to the rest-frame system of the nucleons with  $v_\mu = (1, 0, 0, 0)$ . Notice that the term  $N^\dagger \delta m_N N$  enters the Lagrangian  $\mathcal{L}_{\pi N}^{(2)}$  as a consequence of using the physical nucleon mass instead of the bare one. Further, we have not included the term  $-1/(4F^2) N^\dagger \boldsymbol{\tau} \cdot (\boldsymbol{\pi} \times \dot{\boldsymbol{\pi}}) N$  in the effective Lagrangian  $\mathcal{L}_{\pi N}^{(1)}$ , which results from the covariant derivative of the nucleon field in the third line of eq. (2.22). As already explained above, the corresponding contributions to the OPE vanish since an odd power of the loop momentum  $l$  to be integrated over enters the explicit expressions. Finally,

<sup>#13</sup>Pion loops start to contribute at next higher order in the chiral expansion.

it should be kept in mind that the effective Lagrangian (2.61) is expressed in terms of renormalized pion fields, which leads to the additional contribution with an insertion of  $\delta Z_\pi$  in  $\mathcal{L}_{\pi N}^{(3)}$ . The Hamilton density corresponding to eq. (2.61) is given by

$$\begin{aligned}
\mathcal{H}_2^0 &= -\tilde{N}^\dagger \frac{\vec{\nabla}^2}{2m_N} \tilde{N}, \\
\mathcal{H}_0 &= \tilde{N}^\dagger \left( \frac{\overset{\circ}{g}_A}{2F} \boldsymbol{\tau} \vec{\sigma} \cdot \vec{\nabla} \boldsymbol{\pi} + \frac{\overset{\circ}{g}_A}{4F^3} (\boldsymbol{\pi} \vec{\sigma} \cdot \vec{\nabla} \boldsymbol{\pi}) \boldsymbol{\tau} \cdot \boldsymbol{\pi} \right) \tilde{N} + \dots, \\
\mathcal{H}_2 &= \tilde{N}^\dagger \left( -\delta m_N^{(3)} + \frac{2M_\pi^2 d_{16}}{F} - \frac{M_\pi^2 d_{18}}{F} + \frac{\overset{\circ}{g}_A}{4F} \delta Z_\pi \right) \boldsymbol{\tau} \vec{\sigma} \cdot \vec{\nabla} \boldsymbol{\pi} \tilde{N} + \dots.
\end{aligned} \tag{2.63}$$

Here we switched to the field  $\tilde{N}$  defined as

$$\tilde{N} = (Z_N^N)^{-1/2} N = \left( 1 - \frac{\delta Z_N^N}{2} \right) = (1 + 4M_\pi^2 \tilde{d}_{28}) N, \tag{2.64}$$

in order to get rid of the time derivative in the third line of eq. (2.61). Further we have used a classification of the vertices in effective Lagrangian different from ref.[2]. To be more precise, the dimension  $\Delta$  of the interaction  $\mathcal{H}_\Delta$  is defined as:

$$\Delta = d + \frac{1}{2}n + l - 2. \tag{2.65}$$

Here  $d$ ,  $n$  and  $l$  is the number of derivatives or insertions of  $M_\pi$ , nucleon field operators and insertions of the factors  $1/m_N$ , respectively. According to the power counting suggested by Weinberg [1] we treat the nucleon mass as a much larger scale compared to  $\Lambda_\chi$  ( $m_N \sim \Lambda_\chi^2/Q$ ). As a consequence, relativistic corrections enter at higher orders compared to the corresponding chiral corrections. Notice further that the nucleon field operators in eq. (2.63) are always taken in the normal ordering. Allowing contractions of nucleons field operators would only lead to shifts in the values of various coupling constants in the effective Lagrangian (Hamiltonian) which are independent of  $M_\pi$  and thus of no importance for our considerations.<sup>#14</sup>

We will now follow the lines of [2] and derive the effective Hamiltonian, which acts on the purely nucleonic subspace of the whole Fock space, using the method of unitary transformation. The idea of this method is described in section 2.1. For a detailed discussion on the way of solving the nonlinear decoupling equation (2.17) and calculating the effective Hamiltonian according to eqs. (2.19),(2.20) the reader is addressed to ref. [2].

Let us begin with the one-nucleon effective Hamiltonian  $\tilde{H}_{1N}$ :

$$\begin{aligned}
\tilde{H}_{1N} &= \tilde{H}_{1N}^{(0)} + \tilde{H}_{1N}^{(1)} + \dots, \\
\tilde{H}_{1N}^{(0)} &= \eta_1 \left( H_2 + A_0^\dagger \lambda^1 H_0 + H_0 \lambda^1 A_0 + A_0^\dagger \lambda^1 \omega A_0 \right) \eta_1 \\
&= \eta_1 \left( H_2 - H_0 \frac{\lambda^1}{\omega} H_0 \right) \eta_1, \\
&\dots,
\end{aligned} \tag{2.66}$$

---

<sup>#14</sup>Remember that one does not start from a normal ordering for pion field operators is required. Pion tadpole diagrams lead to  $M_\pi$ -dependent renormalization of various constants in the effective Lagrangian and thus must be considered explicitly.



where the subscript  $i$  (superscript  $j$ ) of the projector  $\eta_i$  ( $\lambda^j$ ) denotes the number of nucleons (pions) in the corresponding state and  $\omega$  is the pionic free energy. Further,  $H_i$  denote Hamilton operators corresponding to the Hamilton density  $\mathcal{H}_i$  in eq. (2.63). The operator  $\lambda^1 A_0 \eta_1$  is given by [2]:

$$\lambda^1 A_0 \eta_1 = -\frac{\lambda^1}{\omega} H_0 \eta_1. \quad (2.67)$$

The superscript  $\nu$  of  $\tilde{H}_{1N}^{(\nu)}$  refers to the order in the chiral expansion and is defined as:<sup>#15</sup>

$$\nu = -2 + 2E_n + 2(L - C) + \sum_i V_i \Delta_i, \quad (2.68)$$

where  $E_n$ ,  $L$ , and  $C$  denote the number of nucleons, closed loops and separately connected pieces, in order. Furthermore,  $V_i$  is the number of vertices of type  $i$ . Performing straightforward calculations we end up with the following result:

$$h_{1N}^{(0)} = \frac{\vec{p}^2}{2m_N} - \delta m_N^{(3)} - \frac{3 g_A^2}{8F^2} J_{12}, \quad (2.69)$$

where we switched to a more convenient nonrelativistic notation, i.e. we omit creation and annihilation operators as well as summation over the appropriate quantum numbers. To be more precise, the relation between  $H_{1N}$  and  $h_{1N}$  is given by

$$H_{1N} = \sum_\alpha \int d^3p n_\alpha^\dagger(\vec{p}) n_\alpha(\vec{p}) h_{1N}(\vec{p}), \quad (2.70)$$

where  $\alpha$  refers to discrete quantum numbers (spin and isospin) and  $n_\alpha^\dagger(\vec{p})$  ( $n_\alpha(\vec{p})$ ) is a creation (annihilation) operator for the nucleon field. It is now easy to read off the expression for the nucleon mass shift  $\delta m_N$  up to the order considered here:

$$\delta m_N = -4c_1 M_\pi^2 - \frac{3 g_A^2}{8F^2} J_{12}, \quad (2.71)$$

which agrees precisely with the result obtained in the previous section using the covariant perturbation theory. One sees from eq. (2.69) that the leading one-nucleon Hamiltonian is given, in accordance with our expectation, just by the nucleon kinetic energy  $h_{1N}^{(0)} = \vec{p}^2 / (2m_N)$ . Notice that since we are interested in the NN interaction at order  $\nu = 2$ , we should in principle also consider  $h_{1N}^{(2)}$  and thus include higher order nucleon mass shifts. We will, however, see explicitly in what follows that this is not necessary. Moreover, we will show that even the leading shift in nucleon mass,  $\delta m_N^{(2)} = -4c_1 M_\pi^2$ , contributes at NNLO and thus can be neglected.

The nucleon  $Z$ -factor  $Z_N$  needs, in principle, not be calculated separately in the method of unitary transformation, since it already enters eq. (2.20). More precisely, the part of the  $Z$ -factor  $Z_N^\pi$ , which corresponds to dressing of the bare nucleon by virtual pions, is related to the operator  $\eta_1 (1 + A^\dagger A)^{-1/2} \eta_1$ . Indeed, the  $Z$ -factor is given by

$$|\chi_1\rangle = (Z_N^\pi)^{-1/2} |\phi_1\rangle, \quad (2.72)$$

<sup>#15</sup>We use here the definition of the counting index  $\nu$  different from the one introduced in ref. [2]. The presently used notation is more transparent when operators with different number of nucleons, i.e. 1N, 2N, 3N, ... forces, are considered. All results of ref. [2] remain however unchanged.

where  $|\phi_1\rangle$  is the original (bare) one–nucleon state and  $|\chi_1\rangle$  is the properly normalized one–nucleon state (i.e. which satisfies the orthonormality condition as described in section 2.1). It follows from eqs. (2.72),(2.18) that:

$$\begin{aligned} (Z_N^\pi)^{-1/2} &\equiv \langle \phi_1 | \chi_1 \rangle = \langle \phi | \eta_1 (1 + A^\dagger A)^{1/2} \eta_1 | \phi \rangle \\ &= \langle \phi | \eta_1 \left( 1 + \frac{1}{2} A_0^\dagger \lambda^1 A_0 + \dots \right) \eta_1 | \phi \rangle = 1 + \frac{3 \overset{\circ}{g}_A^2}{16F^2} J_{13} + \dots \end{aligned} \quad (2.73)$$

The complete nucleon  $Z$ –factor  $Z_N$ , which is related to the specific choice of nucleon field made in the Lagrangian (2.61), is given by (at the order considered)

$$Z_N = Z_N^N Z_N^\pi = 1 - 8M_\pi^2 \tilde{d}_{28} - \frac{3 \overset{\circ}{g}_A^2}{8F^2} J_{13}. \quad (2.74)$$

This agrees with  $Z_N$  from eq. (2.31). We should, however, stress that the  $Z$ –factor is not an observable quantity and depends on the choice of fields. For example, there would be no contribution proportional to  $\tilde{d}_{28}$  in  $Z_N$  if we had decided to work with the fields  $\tilde{N}$  instead of  $N$ . For more discussion on the role of the nucleon  $Z$ –factor in the old–fashioned perturbation theory and Hamiltonian formalism the reader is referred to [21, 20, 31, 32, 33] (for corresponding discussions in the framework of baryon CHPT, see e.g. [34, 35]).

Let us now consider the 2N effective Hamiltonian at order  $\nu = 2$ . The explicit operators at NLO are

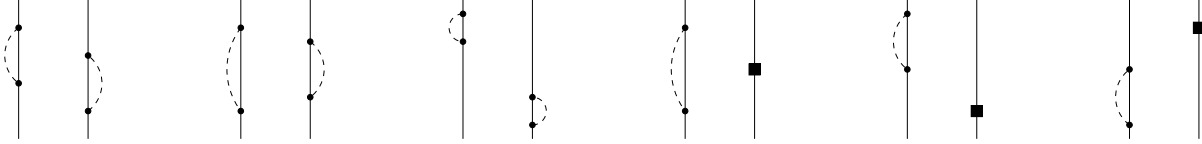


Figure 4: Contributions to the two–nucleon Hamiltonian at order  $\nu = 2$ : disconnected graphs. Heavy dots refer to the leading order  $\pi NN$  vertex of dimension  $\Delta = 0$  while the solid rectangles correspond to insertions of the vertex with  $\Delta = 2$ . For remaining notation see fig. 1.

given in ref. [2]. For our purposes we do not need all terms but only the following ones:

$$\begin{aligned} h_{2N}^{(2)} &= \eta_2 \left( -H_0 \frac{\lambda^1}{\omega} H_0 \frac{\lambda^2}{\omega_1 + \omega_2} H_0 \frac{\lambda^1}{\omega} H_0 + \frac{1}{2} H_0 \frac{\lambda^1}{(\omega)^2} H_0 \eta_2 H_0 \frac{\lambda^1}{\omega} H_0 + \frac{1}{2} H_0 \frac{\lambda^1}{\omega} H_0 \eta_2 H_0 \frac{\lambda^1}{(\omega)^2} H_0 \right. \\ &\quad \left. + H_0 \frac{\lambda^1}{\omega} H_2 \frac{\lambda^1}{\omega} H_0 - \frac{1}{2} H_0 \frac{\lambda^1}{(\omega)^2} H_0 \eta_2 H_2 - \frac{1}{2} H_2 \eta_2 H_0 \frac{\lambda^1}{(\omega)^2} H_0 \right) \eta_2. \end{aligned} \quad (2.75)$$

In fig. 4 we show disconnected diagrams, which contribute to the 2N effective Hamiltonian at order  $\nu = 2$ , which do not include the nucleon self–energy.<sup>#16</sup> Denoting by  $\mathcal{M}$  the common spin–isospin

<sup>#16</sup>Notice that the third diagram in fig. 4 is related to the last two operators in the first line of eq. (2.75) and thus does not correspond to the iteration of the nucleon self–energy contribution. The same holds true for last two graphs in this figure.

structure as well as the loop integrals and using the first line of eq. (2.75) we see that the contribution of the first three diagrams in fig. 4 vanishes:

$$\mathcal{M} \left( -\frac{2}{\omega_1^2 \omega_2^2 (\omega_1 + \omega_2)} - \frac{1}{\omega_1^3 \omega_2 (\omega_1 + \omega_2)} - \frac{1}{\omega_1 \omega_2^3 (\omega_1 + \omega_2)} + \frac{1}{\omega_1^3 \omega_2^2} + \frac{1}{\omega_1^2 \omega_2^3} \right) = 0 \quad (2.76)$$

A similar cancellation is also observed for the remaining graphs in fig. 4 using the second line of eq. (2.75). Thus no disconnected diagrams (which are different from the nucleon self energy graphs) contribute to the NN potential at NLO.

Consider now the diagrams shown in fig.5, which are of the same topology as Feynman graphs 1–4 in fig. 2. The corresponding operators are given in eq. (2.75). Note that the contribution of the diagrams

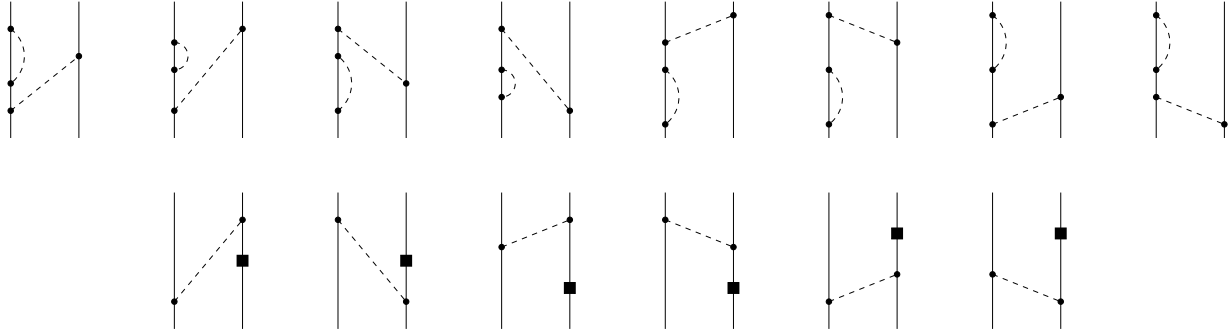


Figure 5: Contributions to the OPE at order  $\nu = 2$ . For notation see fig. 4.

in the lower row in fig. 5 vanishes similarly to the previously considered case of disconnected graphs. Performing explicit calculations one finds the same result as in the covariant approach, namely:<sup>#17</sup>

$$h_{2N}^{(2)} = Z_N \tilde{\mathcal{A}}_{\text{OPE}}^{\text{NC}}, \quad (2.77)$$

where  $Z_N$  is given in eq. (2.31). The OPE amplitude  $\tilde{\mathcal{A}}_{\text{OPE}}^{\text{NC}}$  is the same as  $\mathcal{A}_{\text{OPE}}^{\text{NC}}$  in eq. (2.27) with the only difference that the physical pion mass  $M_\pi$  is used instead of  $M$  (since we are working now with renormalized pion fields). We will not consider the topologies related to graphs 5 and 6 in fig. 2, since the corresponding contributions vanish as explained above. The remaining contributions to the OPE at NLO in the method of unitary transformation are depicted in fig. 6. The first four diagrams show all possible time orderings of the covariant graph 7 of fig. 2 and correspond to the first operator in eq. (2.75). Explicit evaluation leads to the same expression as found in the covariant approach, see eq. (2.37):

$$h_{2N}^{(2)} = Z_7 \tilde{\mathcal{A}}_{\text{OPE}}^{\text{NC}}, \quad Z_7 = -\frac{\overset{\circ}{g}_A^2}{4F^2} \left( 1 - d + \frac{2}{d-1} \right) J_{13}. \quad (2.78)$$

The two pion tadpole diagrams in fig. 6 result from contracting two pion field operators when expressing the term  $-\tilde{N}^\dagger \frac{\overset{\circ}{g}_A}{4F^3} (\boldsymbol{\pi} \vec{\sigma} \cdot \vec{\nabla} \boldsymbol{\pi}) \boldsymbol{\tau} \cdot \boldsymbol{\pi} \tilde{N}$  from eq. (2.63) in normal ordered form, as it also happened in case

<sup>#17</sup>In order to be consistent with the results of the previous section we give here and in what follows explicit expressions for the effective Hamiltonian based upon the nucleon field  $N$ , which is related to  $\tilde{N}$  via eq. (2.64). As a consequence, we have to take into account the additional normalization factor  $(Z_N^N)^{-1/2}$ .

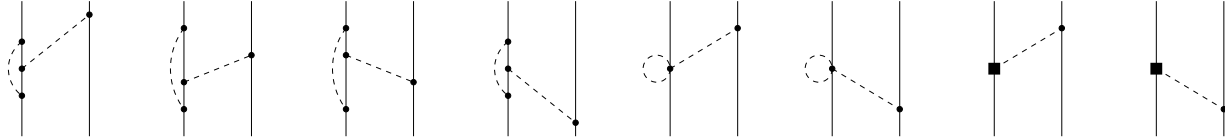


Figure 6: Remaining contributions to the OPE at order  $\nu = 2$ . For notation see fig. 4.

of the pion self-energy discussed above. A straightforward but somewhat tedious calculation leads again to the same result as in the covariant approach:

$$h_{2N}^{(2)} = Z_8 \tilde{\mathcal{A}}_{\text{OPE}}^{\text{NC}}, \quad Z_8 = \frac{1}{2F^2} J_{01}. \quad (2.79)$$

Consider now the last two diagrams in fig. 6. Since we have chosen to work with renormalized pion field operators in the method of unitary transformation, we have no diagrams corresponding to graphs 10 and 11 in fig. 2. Contributions of these two graphs are now taken into account by using the physical pion mass  $M_\pi$  instead of  $M$  as well as by an additional interaction proportional to  $\delta Z_\pi$  in the last line of eq. (2.63). For the last two diagrams in fig. 6 we thus find:

$$h_{2N}^{(2)} = \left( \delta Z_\pi + \frac{8M^2 d_{16}}{\overset{\circ}{g}_A} - \frac{4M^2 d_{18}}{\overset{\circ}{g}_A} \right) \tilde{\mathcal{A}}_{\text{OPE}}^{\text{NC}}. \quad (2.80)$$

Summing up all corrections to the OPE in the method of unitary transformation we end up with the same expression (2.42) as found from covariant perturbation theory using the S-matrix methods.

In summary, we have shown how to perform renormalization in the method of unitary transformation. We recover the same expressions for pion and nucleon mass shifts as well as for corresponding  $Z$ -factors. We have further demonstrated that the NLO OPE potential derived using the method of unitary transformation, where the unitary operator is chosen according to eq. (2.21), coincides with the off-the-energy shell extension of the S-matrix. The TPE contribution has already been considered in both approaches, see refs.[16, 2, 3] and identical results have been reported as well. We do not need to reconsider the TPE contributions and the pion loop diagrams which renormalize the short-range terms since no pion tadpoles appear in those cases and the results of refs.[2, 3] can be adopted without any changes.

## 2.4 Explicit expressions for the potential at NLO

We now give the explicit expressions for the chiral effective NN potential  $V_{\text{NLO}}$ , which we use for extrapolation in the pion mass:

$$V_{\text{NLO}} = V^{\text{OPE}} + V^{\text{TPE}} + V^{\text{cont}}, \quad (2.81)$$

where

$$V^{\text{OPE}} = -\frac{1}{4} \frac{g_A^2}{F_\pi^2} \left( 1 + 2\Delta - \frac{4\tilde{M}_\pi^2}{g_A} \bar{d}_{18} \right) \boldsymbol{\tau}_1 \cdot \boldsymbol{\tau}_2 \frac{(\vec{\sigma}_1 \cdot \vec{q})(\vec{\sigma}_2 \cdot \vec{q})}{\vec{q}^2 + \tilde{M}_\pi^2}, \quad (2.82)$$

$$V^{\text{TPE}} = -\frac{\boldsymbol{\tau}_1 \cdot \boldsymbol{\tau}_2}{384\pi^2 f_\pi^4} \left\{ L(q) \left[ 4\tilde{M}_\pi^2(5g_A^4 - 4g_A^2 - 1) + \vec{q}^2(23g_A^4 - 10g_A^2 - 1) + \frac{48g_A^4 \tilde{M}_\pi^4}{4\tilde{M}_\pi^2 + \vec{q}^2} \right] + \vec{q}^2 \ln \frac{\tilde{M}_\pi}{M_\pi} (23g_A^4 - 10g_A^2 - 1) \right\} \quad (2.83)$$

$$- \frac{3g_A^4}{64\pi^2 f_\pi^4} \left( L(q) + \ln \frac{\tilde{M}_\pi}{M_\pi} \right) \left\{ \vec{\sigma}_1 \cdot \vec{q} \vec{\sigma}_2 \cdot \vec{q} - \vec{q}^2 \vec{\sigma}_1 \cdot \vec{\sigma}_2 \right\},$$

$$V^{\text{cont}} = \bar{C}_S + \bar{C}_T(\vec{\sigma}_1 \cdot \vec{\sigma}_2) + \tilde{M}_\pi^2 \left( \bar{D}_S - \frac{3g_A^2}{32\pi^2 F_\pi^4} (8F_\pi^2 C_T - 5g_A^2 + 2) \ln \frac{\tilde{M}_\pi}{M_\pi} \right) \quad (2.84)$$

$$+ \tilde{M}_\pi^2 \left( \bar{D}_T - \frac{3g_A^2}{64\pi^2 F_\pi^4} (16F_\pi^2 C_T - 5g_A^2 + 2) \ln \frac{\tilde{M}_\pi}{M_\pi} \right) (\vec{\sigma}_1 \cdot \vec{\sigma}_2)$$

$$+ C_1 \vec{q}^2 + C_2 \vec{k}^2 + (C_3 \vec{q}^2 + C_4 \vec{k}^2) (\vec{\sigma}_1 \cdot \vec{\sigma}_2)$$

$$+ iC_5 \frac{\vec{\sigma}_1 + \vec{\sigma}_2}{2} \cdot (\vec{k} \times \vec{q}) + C_6 (\vec{q} \cdot \vec{\sigma}_1) (\vec{q} \cdot \vec{\sigma}_2) + C_7 (\vec{k} \cdot \vec{\sigma}_1) (\vec{k} \cdot \vec{\sigma}_2),$$

with  $g_A$  and  $F_\pi$  the physical values of the nucleon axial coupling and pion decay constant, respectively. Here and in what follows we denote the value of the pion mass by  $\tilde{M}_\pi$  in order to distinguish it from the physical one denoted by  $M_\pi$ . Further,

$$L(q) \equiv L(|\vec{q}|) = \frac{\sqrt{4\tilde{M}_\pi^2 + \vec{q}^2}}{|\vec{q}|} \ln \frac{\sqrt{4\tilde{M}_\pi^2 + \vec{q}^2} + |\vec{q}|}{2\tilde{M}_\pi}, \quad (2.85)$$

and  $\Delta$  represents the relative shift in the ratio  $g_A/F_\pi$  compared to its physical value:

$$\Delta \equiv \frac{(g_A/F_\pi)_{\tilde{M}_\pi} - (g_A/F_\pi)_{M_\pi}}{(g_A/F_\pi)_{M_\pi}} \quad (2.86)$$

$$= \left( \frac{g_A^2}{16\pi^2 F_\pi^2} - \frac{4}{g_A} \bar{d}_{16} + \frac{1}{16\pi^2 F_\pi^2} \bar{l}_4 \right) (M_\pi^2 - \tilde{M}_\pi^2) - \frac{g_A^2 \tilde{M}_\pi^2}{4\pi^2 F_\pi^2} \ln \frac{\tilde{M}_\pi}{M_\pi}. \quad (2.87)$$

Note that in the TPEP we only take into account the explicit  $M_\pi$ -dependence and use the physical values for  $g_A$  and  $F_\pi$ . This is perfectly sufficient at NLO since any shift in  $g_A$  and  $F_\pi$  for a different value of  $M_\pi$  in the TPE is a N<sup>4</sup>LO effect. We have expressed the potential in eqs. (2.82)–(2.84) in such a way that it coincides for  $\tilde{M}_\pi = M_\pi$  with the one given in [3].<sup>#18</sup> The constants  $\bar{C}_{S,T}$  and  $\bar{D}_{S,T}$  are related to the  $C_{S,T}$  from [3] via

$$C_{S,T} = \bar{C}_{S,T} + M_\pi^2 \bar{D}_{S,T}. \quad (2.88)$$

Note further that the short-range terms of the type  $\tilde{M}_\pi^2 \ln \tilde{M}_\pi$  in eq. (2.84) result from the two-pion exchange as well as from the renormalization of the leading-order contact forces by pion loops. It is important to stress that renormalization of the LECs  $C_S$ ,  $C_T$ ,  $C_{1,\dots,7}$  due to pion loops does not depend on the pion mass and thus is of no relevance for this work.

We will now briefly discuss an important issue related to the renormalization of the NN potential. We have performed the calculation of the renormalized OPE in the previous section without specifying a regularization scheme and gave only general (unregularized) expressions. One might worry about

<sup>#18</sup>The term in eq. (2.82) which breaks the Goldberger–Treiman relation and is proportional to  $\bar{d}_{18}$  is not shown explicitly in ref. [3].

the dependence of the results on the regularization scheme. Let us consider as a simple example the nucleon mass shift in eq. (2.71). Applying dimensional regularization to the divergent integral  $J_{12}$  one ends up with the finite shift given by eq. (2.34). The bare nucleon mass  $\overset{\circ}{m}$  in that case is finite and the constant  $c_1$  is not renormalized. Similarly, some other bare quantities like  $M$ ,  $F$ ,  $\overset{\circ}{g}_A$  are finite. The situation might change if a different regularization scheme is applied. For example, performing a momentum cut-off regularization of  $J_{12}$  in eq. (2.71) one finds:

$$\delta m_N = -4c_1 M_\pi^2 - \frac{3\overset{\circ}{g}_A^2}{8F^2} J_{12} = -4c_1 M_\pi^2 - \frac{3\overset{\circ}{g}_A^2}{8F^2} \left( \alpha \Lambda^3 + \beta M_\pi^2 \Lambda + \frac{M_\pi^3}{4\pi} + \mathcal{O}(\Lambda^{-1}) \right), \quad (2.89)$$

where  $\Lambda$  is the momentum cut-off and the coefficients  $\alpha$  and  $\beta$  depend on the precise choice of the regulator. Taking the limit  $\Lambda \rightarrow \infty$  and performing a redefinition of the constants  $\overset{\circ}{m}$ ,  $c_1$  in order to absorb the terms proportional to  $\Lambda^3$  and  $\Lambda$ , we obtain the same finite shift  $-3\overset{\circ}{g}_A^2 M_\pi^3/(32\pi F^2)$  as in the case of dimensional regularization. The difference to the previously discussed case is that the bare nucleon mass and the bare constant  $c_1$ , which do not correspond to observable quantities, are now infinite. Also other bare parameters are infinite if the cut-off regularization is used, see e.g. refs. [36, 37]. It is, however, crucial to understand that, say, the shift in the nucleon mass from its observed value to the one in the chiral limit is a well defined and finite quantity and is not affected by a specific choice of the regularization scheme. The same holds true for  $F_\pi$  and  $g_A$ . Therefore, we are free to adopt the results for the corresponding shifts in these constants found in CHPT analyses of various processes and based upon the dimensional regularization (i.e. we can use the values for the LECs in eq. (2.86)). We will specify the numerical values of the appropriate LECs in the next section. To close this section let us make a comment on calculating various observables based upon the effective potential introduced above. The NN phase shifts are obtained using the T-matrix method. The corresponding partial-wave projected Lippmann-Schwinger equation reads:

$$T_{l,l'}^{sj}(p', p) = V_{l,l'}^{sj}(p', p) + \sum_{l''} \int \frac{d^3q}{(2\pi)^3} V_{l,l''}^{sj}(p', q) \frac{m_N}{p^2 - q^2 + i\epsilon} T_{l'',l'}^{sj}(q, p). \quad (2.90)$$

Notice that the nucleon mass enters the expression for the two-nucleon propagator in the above equation. Thus apart from the explicit and implicit  $\tilde{M}_\pi$ -dependence of the NN force, which has been discussed above, one should, in principle, take into account the  $\tilde{M}_\pi$ -dependence of  $m_N$  in the Lippmann-Schwinger equation. Since the nucleon mass  $m_N$  is treated in the Weinberg power counting formally as a much larger scale compared to  $\lambda_\chi$  (i.e.  $m_N \sim \Lambda_\chi^2/Q$ ), the shift in the nucleon mass gives the correction to the T-matrix which is suppressed by 3 powers of the small momentum scale and thus contribute at NNLO:

$$m_N = m_N^{\text{CL}} + 4c_1^r M_\pi^2 + \dots = m_N^{\text{CL}} \left( 1 + \frac{4c_1 M_\pi^2}{m_N^{\text{CL}}} + \dots \right) = m_N^{\text{CL}} + \mathcal{O}\left(\frac{Q^3}{\Lambda_\chi^3}\right), \quad (2.91)$$

where  $m^{\text{CL}}$  refers to the nucleon mass in the chiral limit ( $=\overset{\circ}{m}$  if dimensional regularization is applied). We have checked the above estimation numerically and found indeed a significantly smaller effect in the deuteron binding energy (in the chiral limit) from the nucleon mass shift compared to various contributions at NLO. It goes without saying that the potential  $V(\vec{p}', \vec{p})$  is multiplied by the regulating functions  $f_R(|\vec{p}'|)$ ,  $f_R(|\vec{p}''|)$  in order to cut off the large momentum components in the Lippmann-Schwinger equation (2.90), which cannot be treated properly in effective field theory. We used here the same exponential function  $f_R(|\vec{p}'|) = \exp[-\vec{p}'^4/\Lambda^4]$  as in ref. [4] and vary the cut-off  $\Lambda$  in the range from 500 to 600 MeV.

### 3 Results

#### 3.1 Chiral input and contact terms

For the OPE contribution in eq. (2.82) both explicit and implicit dependences on the pion mass are known, so that a parameter-free extrapolation to values  $\tilde{M}_\pi$  away from the observed one is possible. In what follows, we use  $g_A = 1.26$ ,  $F_\pi = 92.4$  MeV. The constant  $\bar{l}_4$  is fixed from the scalar radius of the pion and the corresponding value is  $\bar{l}_4 = 4.3$  [6]. The LEC  $\bar{d}_{16}$  has recently been determined from the process  $\pi N \rightarrow \pi\pi N$  [38]. In the following we will use the updated value from ref. [39]. To be more specific, we average the values obtained in the 3 different fits in the last reference. This leads to  $\bar{d}_{16} = -1.23$  GeV<sup>-2</sup>. Note that although all values of  $\bar{d}_{16}$  from [39] have the same sign (negative) and are of a similar magnitude, the uncertainty in the determination of this constant remains quite large. We come back to this at the end of this section. The constant  $\bar{d}_{18}$  is fixed from the observed value of the Goldberger–Treiman discrepancy. Using the values of  $g_{\pi N}$  extracted from  $\pi N$  phase shift analysis [40], we get the following value for the LEC  $\bar{d}_{18}$ :  $\bar{d}_{18} = -0.97$  GeV<sup>-2</sup>. Thus we obtain for the ratio  $g_{\pi N}/m_N$ , which is nothing but the strength of the OPE and is related to  $g_A$  and  $F_\pi$  via (at the given order in the chiral expansion)

$$\frac{g_{\pi N}}{m_N} = \frac{g_A}{F_\pi} \left( 1 - \frac{2M_\pi^2}{g_A} \bar{d}_{18} \right), \quad (3.1)$$

the following value in the chiral limit

$$\left( \frac{g_{\pi N}}{m_N} \right)_{\text{CL}} \sim 15.0 \text{ GeV}^{-1}. \quad (3.2)$$

Comparing this value with the physical one of  $13.2 \text{ GeV}^{-1}$ , we conclude that the OPE becomes *stronger* in the chiral limit.

We now turn our attention to the remaining contribution in the NN potential (2.82). The TPE part is parameter-free and the values of the LECs  $C_{1,\dots,7}$  as well as combinations  $\bar{C}_{S,T} + M_\pi^2 \bar{D}_{S,T}$  have already been fixed from the fit to low-energy data in the NN S- and P-waves. Unfortunately, the LECs  $\bar{D}_{S,T}$ , which contribute to S-wave projected potential, are not known at the moment. Ideally, they should be fixed from the  $NN\pi$  system in processes like e.g. pion–deuteron scattering. This has not yet been done. In order to proceed further we assume natural values for these constants, i.e.:

$$\bar{D}_{S,T} = \frac{\alpha_{S,T}}{F_\pi^2 \Lambda_\chi^2}, \quad \text{where } \alpha_{S,T} \sim 1, \quad (3.3)$$

and  $\Lambda_\chi \simeq 1$  GeV. In our analysis in [43] we have shown that **all values** of the dimensionless coefficients  $\alpha$  related to the contact terms lie at NLO in the range  $-2.1 \dots 3.2$  for all cut-offs employed. Thus making the conservative estimate

$$-3.0 < \alpha_{S,T} < 3.0, \quad (3.4)$$

we are rather confident to be on the safe side. Note that this corresponds to the following range for the partial-wave projected values:

$$-\frac{48\pi}{F_\pi^2 \Lambda_\chi^2} < \bar{D}_{1S_0} < \frac{48\pi}{F_\pi^2 \Lambda_\chi^2}, \quad -\frac{24\pi}{F_\pi^2 \Lambda_\chi^2} < \bar{D}_{3S_1} < \frac{24\pi}{F_\pi^2 \Lambda_\chi^2}. \quad (3.5)$$

It is worth mentioning that the term  $\tilde{M}_\pi^2 \bar{D}_T(\vec{\sigma}_1 \cdot \vec{\sigma}_2)$  breaks Wigner symmetry. The value of  $\bar{D}_T$  expected from eq. (3.5) leads to a Wigner symmetry breaking effect that is comparable in size with the one from the observed nonvanishing (leading order) value of  $C_T$  [43] (i.e.  $M_\pi^2 \bar{D}_T \sim C_T$ ), so that the possibility of exact Wigner symmetry in the chiral limit exists. In that case, Wigner symmetry

breaking would be related to the explicit chiral symmetry breaking of QCD. Last but not least, we use here the values of the LEC  $C_{S,T}$ ,  $C_{1,\dots,7}$  from [3].<sup>#19</sup>

Before showing our results for the phase shifts and other quantities, we would like to make a comment on the uncertainty of our extrapolation in  $\tilde{M}_\pi$ . As already pointed out, the main source of uncertainty is related to the unknown values of the LECs  $D_{S,T}$ , which enter the expression for contact interactions at NLO, see eq. (2.84). Although the LECs  $\bar{l}_4$ ,  $\bar{d}_{16,18}$  are known from CHPT analyses of various processes and thus the complete  $\tilde{M}_\pi$ -dependence of the ratio  $g_{\pi N}/m_N$  is fixed at NLO, some uncertainty still remains due to the uncertainty in the determination of the abovementioned LECs. While the constant  $l_4$  is known with relative small error bars, so that the corresponding uncertainty needs not to be discussed here, the LECs  $\bar{d}_{16,18}$  are not known very precisely. Using the values of  $g_{\pi N}$  extracted from three different  $\pi N$  phase shift analyses [41, 40, 42] one gets the values  $\bar{d}_{18} = -1.54 \text{ GeV}^{-2}$ ,  $\bar{d}_{18} = -0.97 \text{ GeV}^{-2}$  and  $\bar{d}_{18} = -0.84 \text{ GeV}^{-2}$ , respectively. From eq. (2.82) one sees that  $\bar{d}_{18}$  does not contribute to the OPE in the chiral limit. Thus at first sight our predictions in the chiral limit seem not to be affected by the uncertainty in this LEC. In fact, this is not quite true, since changing the value of  $\bar{d}_{18}$  leads to a modification of the strength of the OPE at the physical point ( $\tilde{M}_\pi = M_\pi$ ). Therefore, one should, in principle, refit at the same time the LECs  $C_{S,T}$ ,  $C_{1,\dots,7}$  in order to describe the corresponding phase shifts. Modifying the LECs related to the contact interactions would change observables even in the chiral limit. However, we have checked that the corresponding effects in observables are small and will not discuss this issue in what follows. The uncertainty in the LEC  $\bar{d}_{16}$  turns out to be much more important for our analysis. Contrary to the previously discussed case with the LEC  $\bar{d}_{18}$ , changing  $\bar{d}_{16}$  result in changes of the strength of the OPE in the chiral limit (and, of course, for other values of  $\tilde{M}_\pi \neq M_\pi$ ) but does not affect it at the physical point where  $\tilde{M}_\pi = M_\pi$ . In what follows we will demonstrate how the uncertainty in  $\bar{d}_{16}$  shows up in various observables.

### 3.2 Phase shifts

After the remarks of the preceding section we are now in the position to present results. In figs. 7 to 10 we show our predictions for various phase shifts in the chiral limit compared to their values in the real world. In order to estimate the uncertainty due to missing higher order terms we proceed in a usual way and vary the cut-off between 500 and 600 MeV, as it has been done in [4]. The only exception to this are the  $^1S_0$  and  $^3S_1 - ^3D_1$  channels in the chiral limit, where the dark shaded bands in figs.7,8,9 are due to the uncertainty in the values of  $\bar{D}_{S,T}$ . Varying the cut-off in that case is not necessary, since the corresponding uncertainty is much smaller than the one due to unknown  $\bar{D}_{S,T}$ . For these channels we will take the cut-off  $\Lambda = 560 \text{ MeV}$ .

Both S-wave phase shifts in fig. 7 show a qualitatively similar behaviour to what is observed in the real world. In the  $^1S_0$  channel the interaction in the chiral limit gets weaker and the phase shift reaches in the maximum about 30 – 50% of the observed value. The situation in the  $^3S_1$  channel is just opposite but the effect is smaller in magnitude. Note that the band for the  $^1S_0$  phase shift is much wider, partially due to the larger uncertainty in  $\bar{D}_{1S_0}$  compared to the one in  $\bar{D}_{3S_1}$ .

Before considering higher partial waves some comments are in order. First of all we note that the form of the OPE in the chiral limit

$$(V^{\text{OPE}})_{\text{CL}} \propto \frac{(\vec{\sigma}_1 \cdot \vec{q})(\vec{\sigma}_2 \cdot \vec{q})}{\vec{q}^2} \quad (3.1)$$

<sup>#19</sup>In our earlier work [3] we used a value for the pion-nucleon coupling  $g_{\pi N}$ , which is slightly smaller than the commonly accepted one  $g_{\pi N} = 13.1 \dots 13.4$ . We have refitted the contact terms  $C_{S,T}$ ,  $C_{1,\dots,7}$  using the value for  $g_{\pi N}$  according to eq. (3.1). This leads to minor changes in the values of the LECs related to contact terms and does not visibly change observables.



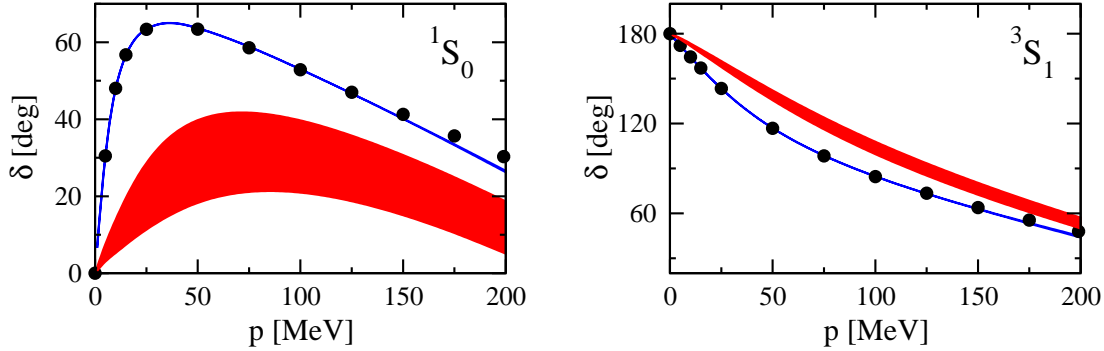


Figure 7: S-wave phase shifts as functions of the momentum in the c.m. system. Dark shaded bands correspond to our NLO predictions in the chiral limit, light shaded bands are NLO results for physical value of  $M_\pi$ , filled circles are Nijmegen phase shifts [30].

leads to significant scattering at vanishing momenta for all partial waves, as pointed out in by Bulgac et al. [10]. It is amusing to note that although the interaction between pions and nucleons vanishes in the chiral limit at vanishing momenta, the interaction between nucleons via the exchange of pions, becomes, on the contrary, stronger as a consequence of the increased range of the interaction for  $\tilde{M}_\pi \rightarrow 0$ .<sup>#20</sup> As a consequence of the vanishing pion mass the effective range expansion

$$k^{2l+1} \cot \delta_l(k) = -\frac{1}{a_l} + r_l \frac{k^2}{2} + v_l^2 k^4 + \dots, \quad (3.2)$$

where  $k$  is the c.m. momentum and  $l$  the angular momentum, does not exist any more. The partial wave amplitude  $A_l(E)$ ,  $E = k^2/m_N$ , describing elastic NN scattering has a left-hand cut starting at the branch point  $E = -\tilde{M}_\pi^2/(4m_N)$ , which gives a maximal radius of convergence of the effective range expansion. Thus the domain of validity of the effective range expansion ceases to exist for  $\tilde{M}_\pi \rightarrow 0$ . Projecting the OPE in the chiral limit, eq. (3.1), onto the states with definite  $l$ ,  $s$  and  $j$  we note that all spin-singlet matrix elements vanish. Further, on-the-energy shell matrix elements in all other channels do not depend on the momenta. As a consequence, one expects that the phase shifts at low energy in the high partial waves, in which the amplitude is essentially given by the Born term and strongly dominated by the OPEP, behave like  $\delta(k) \propto k$ .

Let us now comment on the P-waves which are, as already pointed out in the introduction, of a particular interest, because of the possible existence of bound states due to the strong OPE in the chiral limit. First, we stress that we are able to perform an accurate extrapolation in the pion mass for P- and higher partial waves since the complete  $\tilde{M}_\pi$ -dependence is known. Our findings confirm the conclusions of [10] that no bound states exist in the P-waves. The phase shift in the  $^3P_0$  channel, which is most sensitive to the OPE and thus is an ideal candidate for the appearance of a bound state, is strongly enhanced compared to the physically relevant case and reaches a maximum of about  $32^\circ$ . The  $^1P_1$  phase shift becomes small and is completely given in the chiral limit by the TPEP and the NLO contact term. Remarkably, one observes strong changes in the mixing angle  $\epsilon_1$ , which is known

<sup>#20</sup>The OPEP behaves at large distances in the chiral limit as  $1/r^3$ .

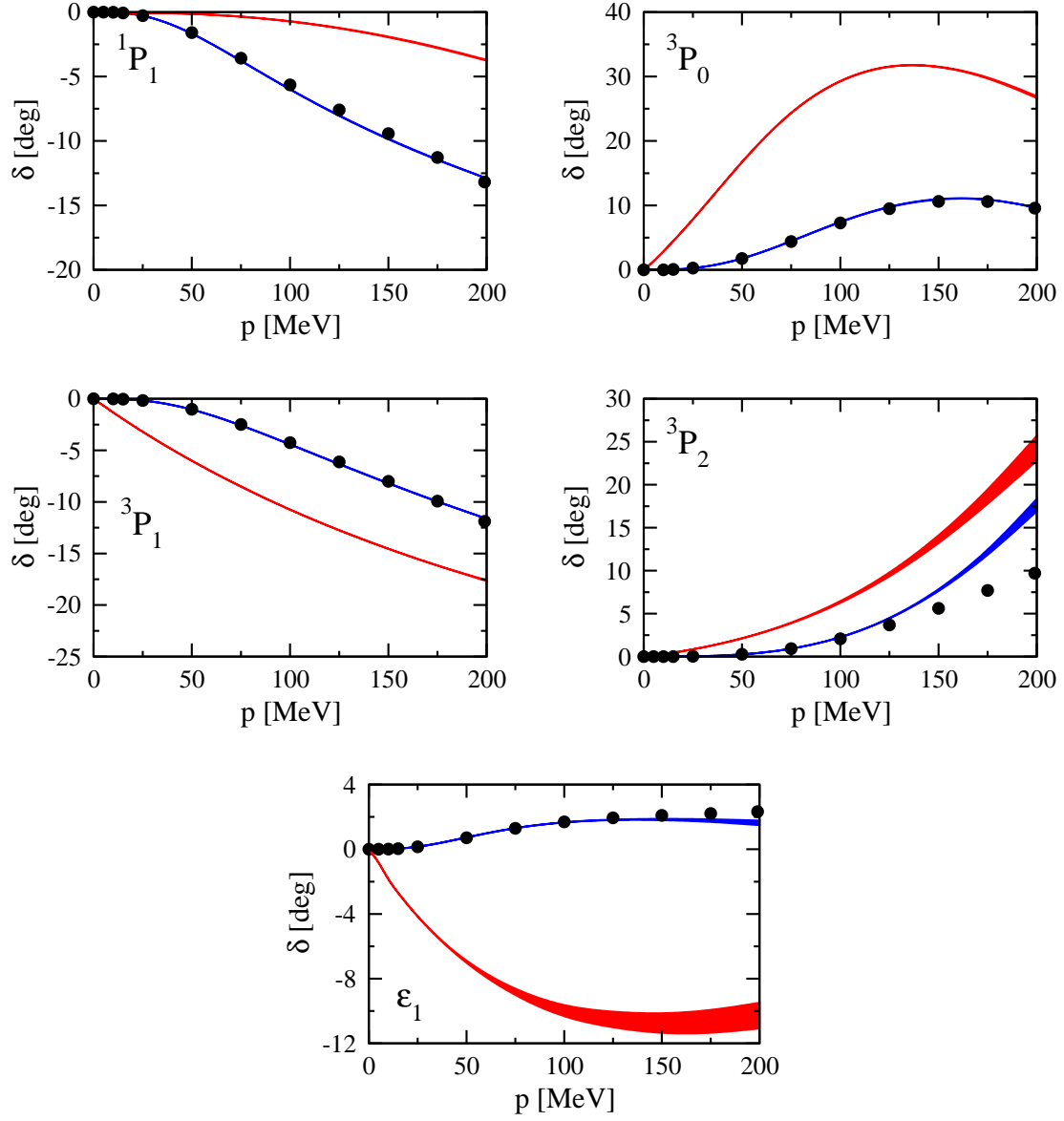


Figure 8: P-wave phase shifts. For notations see fig. 7.

to be an observable that is very sensitive to small changes in certain parameters. It is comforting to note that the bands do not get significantly wider compared to the case with the physical value of the pion mass,  $\tilde{M}_\pi = M_\pi$ . This is a clear indication of the consistency and good quality of the extrapolation to  $\tilde{M}_\pi = 0$ , since the cut-off independence of observables in the chiral limit is achieved by “running” of the LECs  $C_i(\Lambda)$  fixed at the physical value  $\tilde{M}_\pi = M_\pi$ .

The situation with the D- and F- waves turns out to be similar to the case of the P-waves. The phases in most channels (apart from the spin-singlet ones) already follow their asymptotical behaviour discussed above, i.e. grow linearly with momentum  $k$ . Our last comment in this section is that the

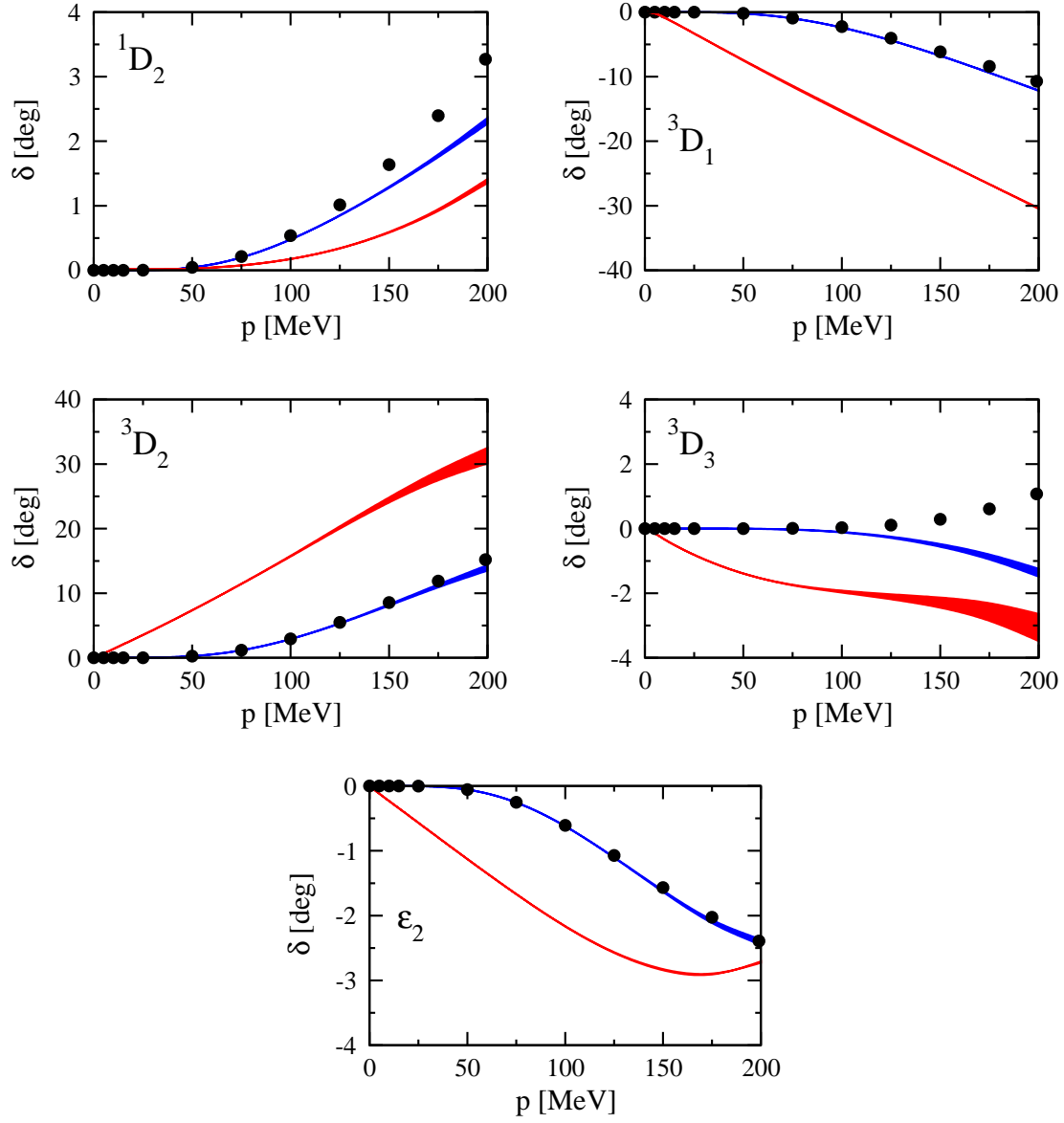


Figure 9: D-wave phase shifts. For notations see fig. 7.

partial wave decomposition becomes not a reasonable (from the practical point of view) tool for calculating observables (full scattering amplitude) if  $M_\pi \rightarrow 0$ , since the expansion in the partial waves converges slowly in the presence of the long-range interaction  $\propto 1/r^3$ .

### 3.3 Deuteron binding energy

We now move on to discuss the deuteron binding energy  $B_D$ , which we consider to be the most interesting observable with respect to its  $\tilde{M}_\pi$ -dependence, see fig. 11. As already pointed out in the introduction, the situation concerning the chiral limit behaviour of  $B_D$  according to the previous

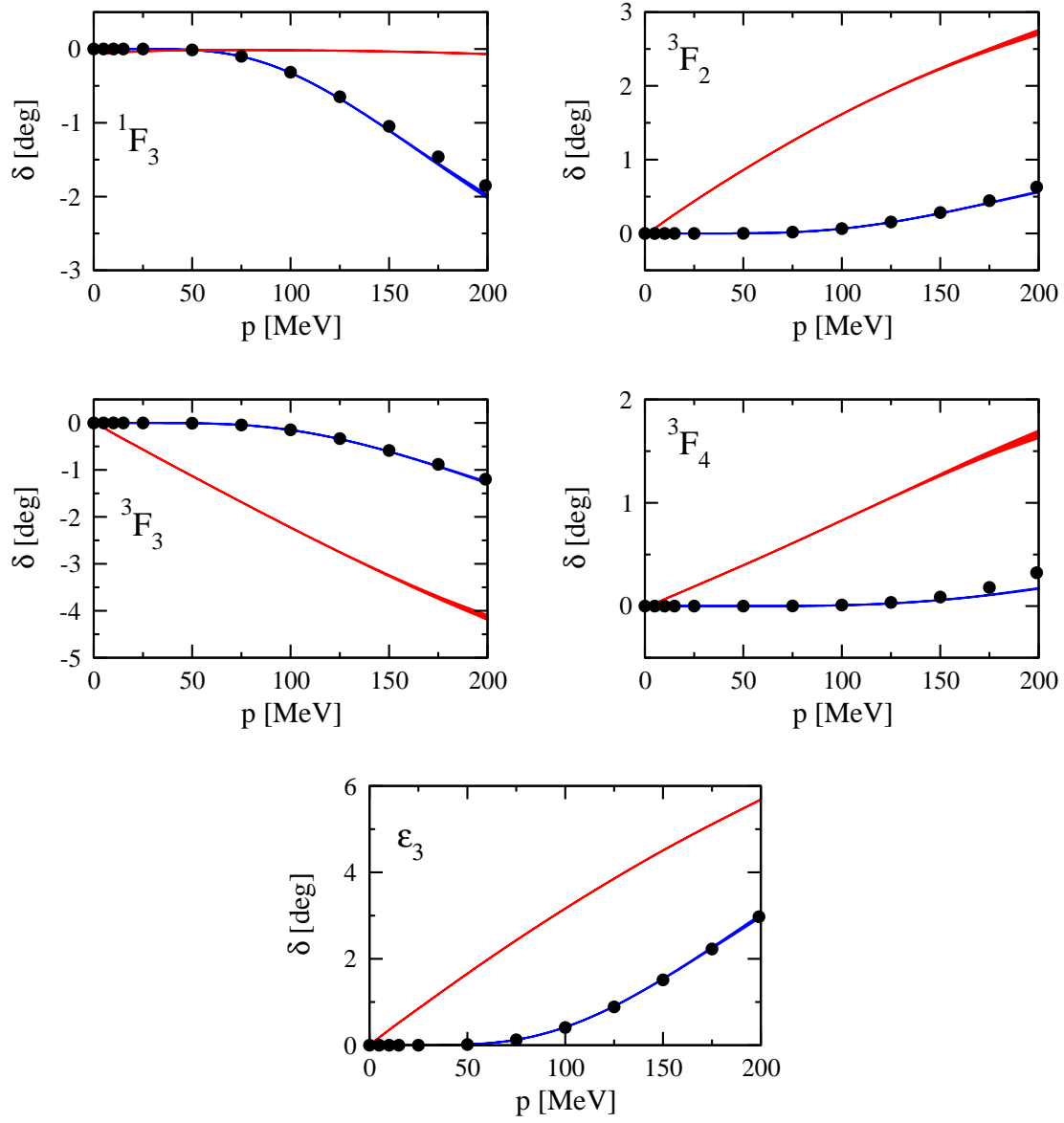


Figure 10: F-wave phase shifts. For notations see fig. 7.

analyses of Bulgac et al. [10] and Beane et al. [11, 14] can not be considered as settled. In fact, the value of  $B_D$  is rather sensitive to the assumptions and approximations made as well as to certain parameters, like the pion-nucleon coupling constant. According to our complete NLO analysis, we arrive at a unique result: the deuteron is *stronger* bound in the chiral limit with the binding energy

$$B_D^{\text{CL}} = 9.6 \pm 1.9 \begin{matrix} +1.8 \\ -1.0 \end{matrix} \text{ MeV}. \quad (3.1)$$

Here, the first error refers to the uncertainty in the value of  $\bar{D}_{3S_1}$ , where the LEC  $\bar{d}_{16}$  is set to the average value  $\bar{d}_{16} = -1.23 \text{ GeV}^{-2}$  from [39]. The second error shows the additional uncertainty when

$\bar{d}_{16}$  is varied in the range given in [39]. We decided not to add these uncertainties but rather give them separately since they are not completely uncorrelated. The value of  $B_D^{\text{CL}}$  is in remarkable agreement with the natural value one would expect to arise in QCD of about  $F_\pi^2/m \sim 10$  MeV, if one (naively) assumes for the binding energy to be of the order of the kinetic energy with the relevant momentum scale being  $p \sim F_\pi$ .<sup>#21</sup>

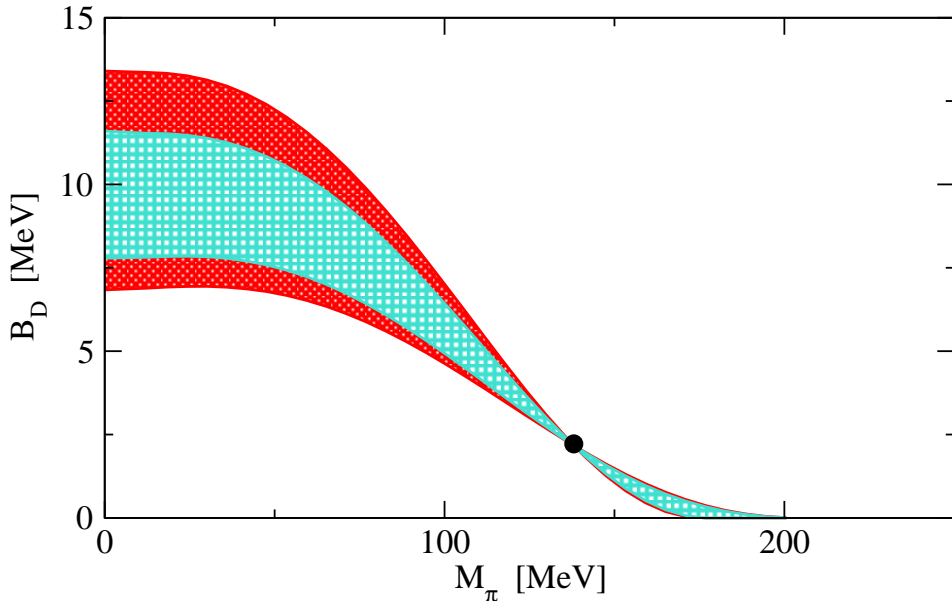


Figure 11: Deuteron binding energy as a function of the pion mass. The shaded areas correspond to allowed values. The light shaded band corresponds to our main result with  $\bar{d}_{16} = -1.23 \text{ GeV}^{-2}$  and the uncertainty due to the unknown LECs  $\bar{D}_{S,T}$ . The dark shaded band gives the uncertainty if, in addition to variation of  $\bar{D}_{S,T}$ , the LEC  $\bar{d}_{16}$  is varied in the range from  $\bar{d}_{16} = -0.91 \text{ GeV}^{-2}$  to  $\bar{d}_{16} = -1.76 \text{ GeV}^{-2}$  given in [39]. The heavy dot shows the binding energy for the physical value of the pion mass.

We also performed extrapolation for larger values of  $\tilde{M}_\pi$ , which might be of interest for later calculations within lattice QCD. According to our analysis the deuteron does not exist anymore for  $\tilde{M}_\pi \gtrsim 200$  MeV. Note that the behaviour of  $B_D$  is qualitatively similar to what has been found in [11] by taking into account only the explicit  $\tilde{M}_\pi$ -dependence.

### 3.4 S-wave scattering lengths and matching with lattice QCD

Our last topic is related to the S-wave scattering lengths  $a^{1S_0}$  and  $a^{3S_1}$  and the possibility of matching with the calculations using lattice QCD. In fig. 12 we show our predictions for the scattering lengths. First of all, it is interesting to see that the uncertainty due to the unknown constant  $\bar{D}_{3S_1}$  does not

<sup>#21</sup>More precisely, one should use in this formula  $F$  and  $\hat{m}$ , but for an approximate estimate the differences to the physical values can be ignored.

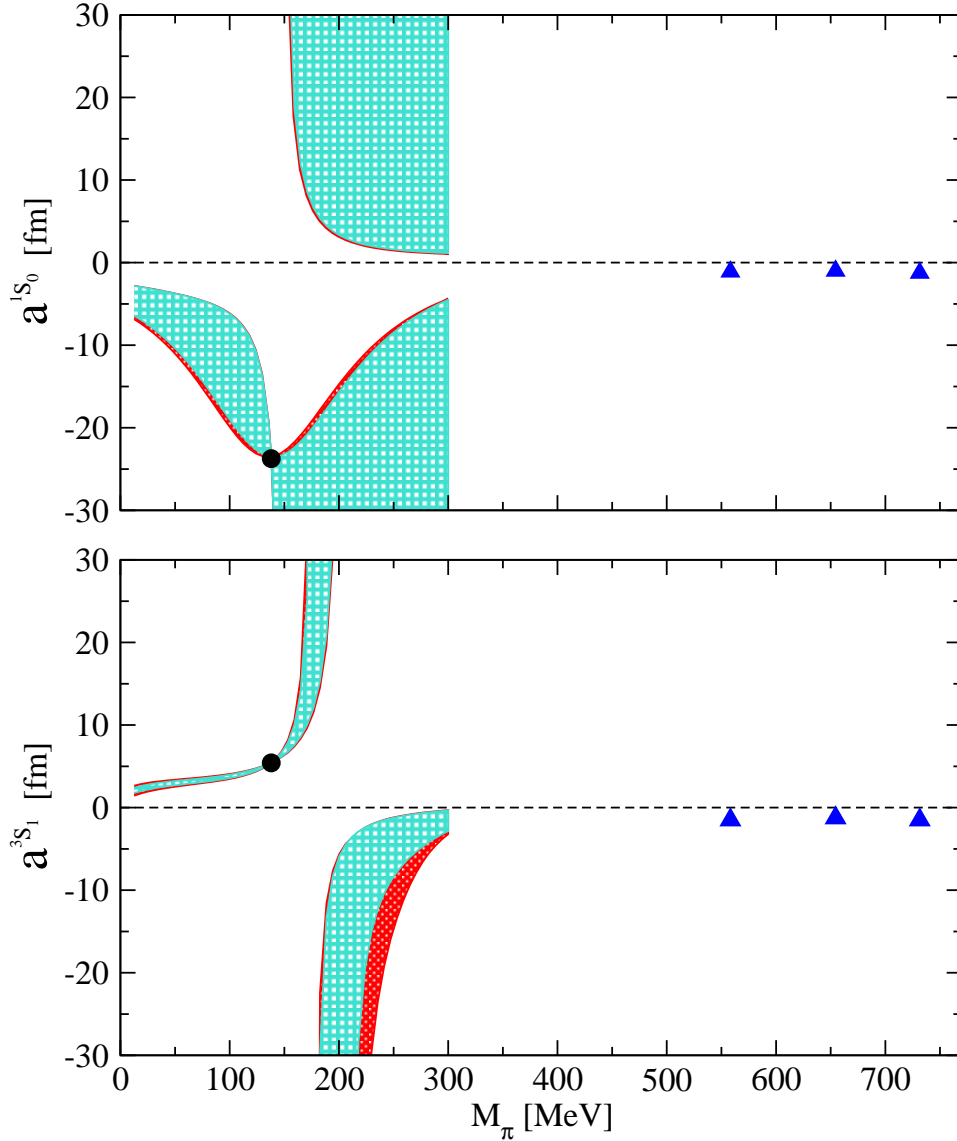


Figure 12: The S-wave scattering lengths as functions of  $\tilde{M}_\pi$ . The shaded areas represent the allowed values according to our analysis. The light shaded band corresponds to our main result with  $\bar{d}_{16} = -1.23 \text{ GeV}^{-2}$  and the uncertainty due to the unknown LECs  $\bar{D}_{S,T}$ . The dark shaded band gives the uncertainty if, in addition to variation of  $\bar{D}_{S,T}$ , the LEC  $\bar{d}_{16}$  is varied in the range from  $\bar{d}_{16} = -0.91 \text{ GeV}^{-2}$  to  $\bar{d}_{16} = -1.76 \text{ GeV}^{-2}$  given in [39]. The heavy dots corresponds to the values in the real world. The triangles refer to lattice QCD results from [13].

show up strongly for  $a^{3S_1}$  for  $\tilde{M}_\pi < M_\pi$ , where we are able to obtain an accurate extrapolation. In the chiral limit the scattering length  $a_{\text{CL}}^{3S_1}$  is still positive and smaller in magnitude compared to the

physically relevant case, which is in agreement with the larger value of the deuteron binding energy. Specifically, we get  $a_{\text{CL}}^{3S_1} = 1.5 \pm 0.4^{+0.2}_{-0.3}$  fm, which is again of natural size. Here the first uncertainty refers to variation in  $\bar{D}_{S,T}$  while the second one to the additional variation in  $\bar{d}_{16}$ , as described above. The scattering length changes its sign at  $\tilde{M}_\pi \sim 200$  MeV and relaxes to natural values for larger  $\tilde{M}_\pi$ . Note also that the relative contribution of the OPE decreases with increasing pion mass and thus the uncertainty due to the variation in  $\bar{d}_{16}$  becomes very small. On the contrary, the uncertainty in  $\bar{D}_{3S_1}$  is, of course, magnified as  $\tilde{M}_\pi$  grows.

In case of the  $a^{1S_0}$  the uncertainty in our extrapolation in the pion mass is visibly larger. This is consistent with the known fact that the OPE plays a less significant role in this channel, where the interaction is dominated by the shorter range terms. Another reason is that an extreme fine tuning leading to the very large value for  $a^{1S_0}$  takes place in the physically relevant case with  $\tilde{M}_\pi = M_\pi$ , where all parameters are fixed. The larger effect due to the uncertainty in the  $\bar{D}_{1S_0}$  thus has to be expected. Nevertheless, our results concerning this channel are also quite interesting. In particular, it turns out that no bound state appears for pion mass smaller than  $M_\pi$ , although in the real world for  $\tilde{M}_\pi = M_\pi$  the virtual state in this channel is almost bound. Around the chiral limit  $a^{1S_0}$  shows a qualitatively similar behaviour to  $a^{3S_1}$  and gets smaller in magnitude:  $a_{\text{CL}}^{1S_0} = -4.1 \pm 1.6^{+0.0}_{-0.4}$  fm, which is still somewhat large compared to what would be expected from dimensional reasons (1 – 2 fm). We are not able to obtain an accurate prediction for  $a^{1S_0}$  for  $\tilde{M}_\pi > M_\pi$ . In that case both scenarios with or without a bound state in this channel are possible. This uncertainty leads to a huge uncertainty with respect to the scattering length, which becomes infinite in the presence of a zero-energy bound state. This situation is depicted in the upper panel of fig. 12. The different signs of the scattering length are due to the fact that the two-nucleon system might be bound or unbound in this channel. It is more appropriate in such a case to look at the inverse scattering length, which simply crosses zero when one encounters a zero energy bound state. We show the inverse scattering lengths  $1/a^{1S_0}$  and  $1/a^{3S_1}$  in fig. 13. Unfortunately, it is not yet possible to compare our extrapolation of the scattering lengths with the results available from the lattice calculation. The latter ones are currently restricted to values of  $\tilde{M}_\pi$  larger than 550 MeV, which is far beyond the domain of applicability of the chiral expansion. Actually, our extrapolation is not trustable anymore for  $\tilde{M}_\pi \gtrsim 2M_\pi$ . For example, the relative shift  $\Delta$  of the ratio  $g_A/F_\pi$  defined in eq. (2.86) reaches  $\sim 50\%$  for  $\tilde{M}_\pi \sim 250$  MeV. Furthermore, the lattice calculation of ref. [13] is carried out in the quenched approximation, so that one, in principle, should perform extrapolation in the pion mass in the quenched chiral perturbation theory, see [44, 45] for more discussion.

### 3.5 Comparison to earlier work

It is interesting to compare our findings with the ones of refs. [11, 14], which are also based on effective field theory. There it was pointed out that the (natural) values of the unknown LECs  $\bar{D}_{S,T}$  exist, which make the deuteron both bound or unbound in the chiral limit and which strongly change the S-wave scattering lengths. Thus no predictions for all these quantities could be made [14]. The basic differences in our analyses can be summarized as follows:

1. While we take the chiral limit value for the strength of the OPE,  $g_A/F_\pi$ , from the CHPT analysis of the  $\pi\pi$ ,  $\pi N$  and  $\pi\pi N$  systems, the authors of ref. [14] make use of the assumption that terms of the type  $M_\pi^2 \ln M_\pi/\Lambda$ , where  $M_\pi \ll \Lambda$  ( $\Lambda \sim M_\rho$ ) dominate the chiral expansion. This leads to a decrease of  $g_A/F_\pi$  in the chiral limit, while the CHPT based analysis gives an increased value. This difference seems to be the most important one.
2. While we take into account the complete TPEP, only its chiral limit value is considered in [14]. In addition, we also include renormalization of the short-range interactions, which leads to the

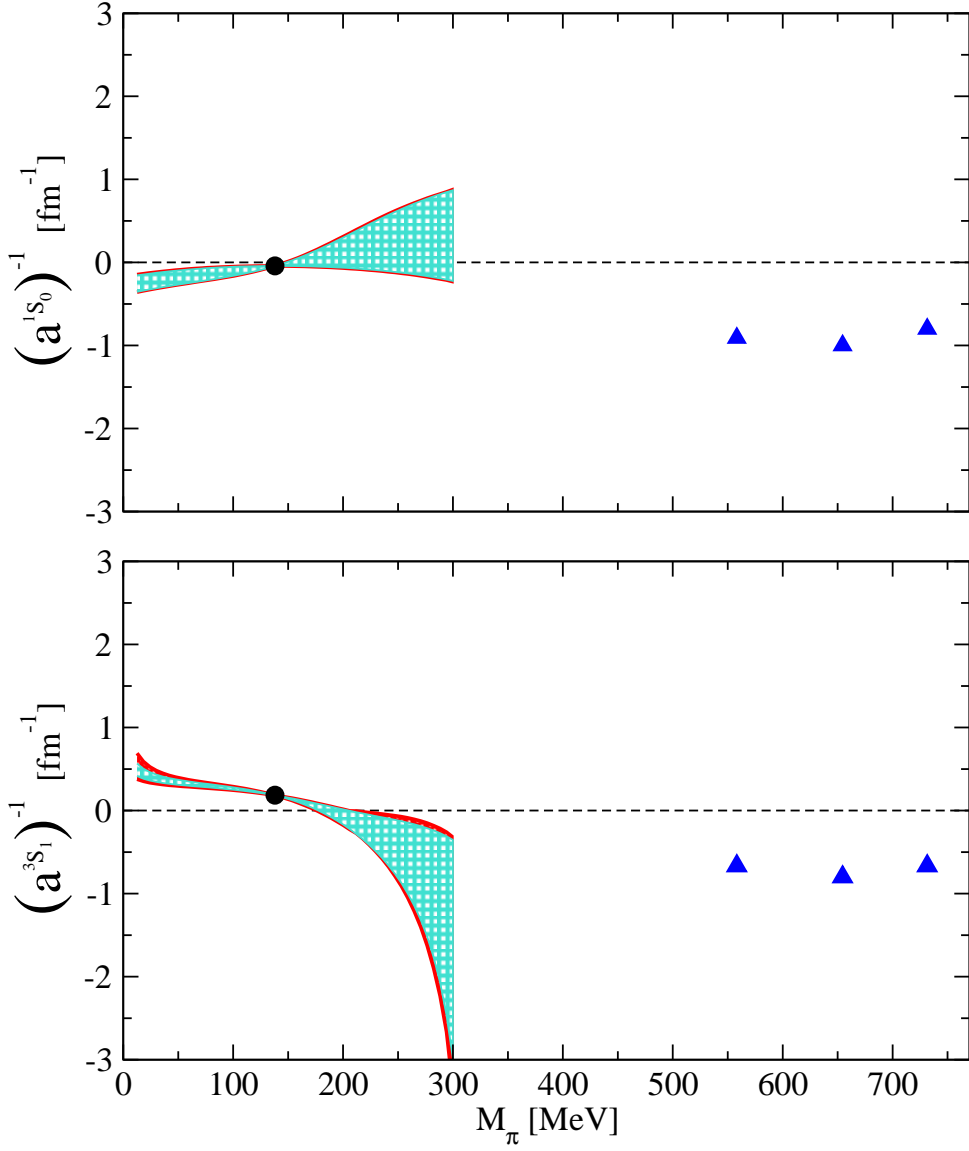


Figure 13: The S–wave inverse scattering lengths as functions of  $\tilde{M}_\pi$ . The shaded areas represent the allowed values according to our analysis. The light shaded band corresponds to our main result with  $\bar{d}_{16} = -1.23 \text{ GeV}^{-2}$  and the uncertainty due to the unknown LECs  $\bar{D}_{S,T}$ . The dark shaded band gives the uncertainty if, in addition to variation of  $\bar{D}_{S,T}$ , the LEC  $\bar{d}_{16}$  is varied in the range from  $\bar{d}_{16} = -0.91 \text{ GeV}^{-2}$  to  $\bar{d}_{16} = -1.76 \text{ GeV}^{-2}$  given in [39]. The heavy dots corresponds to the values in the real world. The triangles refer to lattice QCD results from [13].

nontrivial logarithmic dependence on the pion mass.

3. We regularize the Lippmann–Schwinger in the momentum space by a finite cut–off and do not



require the low-energy phase shifts to be completely but only approximately cut-off independent. The remaining cut-off dependence can be eliminated by inclusion of higher order terms. In [14] the Schrödinger equation in the coordinate space (with the finite short-distance cut-off) is solved. The cut-off independence of the observables is achieved at the expense of introducing short-range interactions in the D-wave, which are not present in the effective Lagrangian.

Finally, we remark that as in ref.[10] we find no new bound states in the P-waves.

## 4 Summary and conclusions

In this paper we have calculated properties of the two-nucleon system in the chiral limit based on a chiral effective field theory. The results of our investigation can be summarized as follows:

- Based upon the modified Weinberg power counting (as explained in [2]) we have shown how to perform a complete renormalization within the method of unitary transformation, including the mass and wave-function renormalization and how to deal with tadpole graphs. We found the renormalized expression for the OPEP within the projection formalism and demonstrated that it agrees precisely with the off-the-energy shell extension of the OPE amplitude obtained in the S-matrix method.
- Based on the NLO potential, which includes the renormalized OPE, TPE contributions and contact terms, we have performed extrapolations in the pion mass (or, equivalently, quark mass) away from its physical value <sup>#22</sup>. The corresponding LECs have been taken from an investigation of  $\pi\pi$  [6],  $\pi N$  [25, 39] and  $NN$  systems [3]. The only uncertainties arise from the unknown couplings  $\bar{D}_{S,T}$  related to contact terms with one insertion  $\sim \tilde{M}_\pi^2$  and to the variation in the pion-nucleon LEC  $\bar{d}_{16}$  related to the Goldberger-Treiman discrepancy. For the dimensionless coefficients that parameterize the LECs  $\bar{D}_{S,T}$  and which are expected to be of order one, we considered values in the range from  $-3$  to  $3$ . The variation in  $\bar{d}_{16}$  is obtained from considering various  $\pi N$  phase shift analyses as input to analyze the process  $\pi N \rightarrow \pi\pi N$ .
- We have calculated the NN phase shifts in the chiral limit. In the  $^1S_0$  and  $^3S_1 - ^3D_1$  channels we obtain predictions with an error governed by the uncertainty in the values of  $\bar{D}_{S,T}$ . Both S-wave phase shifts look qualitatively similar to the physically realized case, although the  $^1S_0$  phase shift is about 50 – 70% smaller in magnitude. The  $^3P_0$  phase shift is enhanced but no bound state appears in that channel, as it is also the case for other P- and higher partial waves. Starting from D- and F-waves, the phase shifts nearly reach their asymptotic behaviour caused by the exchange of a massless pion and grow linearly with momentum,  $\delta(k) \sim k$ .
- According to our analysis, the deuteron is significantly stronger bound in the chiral limit. The binding energy is close to the natural value of  $\sim 10$  MeV one expects to arise in QCD. There is no bound state in the  $^1S_0$  channel in the chiral limit.
- In the chiral limit, the S-wave scattering lengths take smaller (in magnitude) and more natural values as compared to the real world. Furthermore, for pion masses significantly larger than the physical one we found negative values of natural size for the  $^3S_1$  scattering length, which seem to be consistent with the lattice calculation [13]. In the  $^1S_0$  channel the uncertainty due to the unknown LEC  $\bar{D}_{1S_0}$  is much larger than in the triplet channel and we were not able to predict  $a^{1S_0}$  for large values of the pion mass. The scattering length takes both positive and negative

---

<sup>#22</sup>It certainly would be interesting to extend the calculation to NNLO.

values with the magnitude changing from being natural to infinitely large. We also consider inverse scattering lengths, which are more suitable for chiral extrapolation and for comparison with the lattice calculation.

- We have shown that it is possible that Wigner symmetry is also exact in the chiral limit and that its breaking observed in nature is entirely due to the quark mass terms. This would explain why the LECs related to Wigner symmetry breaking turn out to be so much smaller than all other LECs parameterizing the short–distance part of the NN interaction.

To conclude, although we did not find dramatic changes in the properties of the NN systems in the chiral limit, the physically realized value of  $\tilde{M}_\pi$  turns out to be a quite specific one in the sense that it leads to unnaturally large scattering lengths in both S–waves and consequently to the small deuteron binding energy. In fact, nature seems to be more simple in a world with massless quarks since nuclear binding would be of its expected size and the S–wave scattering lengths would be natural. Thus, no fine tuning would be needed and the nuclear force problem would be amenable to a much simpler treatment than required in the real world. Of course, our investigation can not answer the central question why nature chooses such a fine-tuned scenario for the nuclear forces, but at least it is comforting to know that she seems to be more kind in the chiral limit.

## Acknowledgments

We would like to thank Silas Beane and Martin Savage for useful discussions and Nadia Fettes for helpful comments. E.E. would like to thank for the hospitality of the Science Center in Benasque, where a part of this work has been done. This work has been partially supported by the Deutsche Forschungsgemeinschaft (E.E.).

## References

- [1] S. Weinberg, Nucl. Phys. B363 (1991) 3.
- [2] E. Epelbaum, W. Glöckle and Ulf–G. Meißner, Nucl. Phys. A637 (1998) 107.
- [3] E. Epelbaum, W. Glöckle and Ulf–G. Meißner, Nucl. Phys. A671 (2000) 295.
- [4] E. Epelbaum, et al., arXiv:nucl-th/0201064, accepted for publication in Eur. Phys. J. A.
- [5] E. Epelbaum, et al., in preparation.
- [6] J. Gasser, H. Leutwyler, Ann. Phys. 158 (1984) 142.
- [7] S. Bellucci, J. Gasser and M. E. Sainio, Nucl. Phys. B423 (1994) 80 [Erratum-ibid. B431 (1994) 413]; E. Golowich and J. Kambor, Nucl. Phys. B447 (1995) 373; J. Bijnens et al., Phys. Lett. B374 (1996) 210; H. W. Fearing and S. Scherer, Phys. Rev. D53 (1996) 315; P. Post and K. Schilcher, Phys. Rev. Lett. 79 (1997) 4088; J. Bijnens, G. Colangelo and G. Ecker, JHEP 9902 (1999) 020; J. Bijnens, G. Colangelo and G. Ecker, Ann. Phys. 280 (2000) 100.
- [8] S. R. Beane and M. J. Savage, Nucl. Phys. A694 (2001) 511.
- [9] J. P. Uzan, arXiv:hep-ph/0205340.
- [10] A. Bulgac, G.A. Miller, and M. Strikman, Phys. Rev. C56 (1997) 3307.
- [11] S.R. Beane, P.F. Bedaque, M.J. Savage, and U. van Kolck, Nucl. Phys. A700 (2002) 377.
- [12] S.R. Beane, et al., Phys. Rev. A64 (2001) 042103.
- [13] M. Fukugita, et al., Phys. Rev. D52 (1995) 3003.

- [14] S.R. Beane and M.J. Savage, hep-ph/0206113.
- [15] R.J.N. Phillips, Reports on Progress in Physics XXII (1959) 562.
- [16] N. Kaiser, R. Brockmann, and W. Weise, Nucl. Phys. A625 (1997) 758.
- [17] N. Kaiser, Phys. Rev. C61 (2000) 014003, Phys. Rev. C62 (2000) 024001, Phys. Rev. C63 (2001) 044010, Phys. Rev. C64 (2001) 057001, Phys. Rev. C65 (2002) 017001.
- [18] I. Tamm, J. Phys., U.S.S.R., 9 (1945) 449.
- [19] S.M. Dancoff, Phys. Rev. 78 (1950) 382.
- [20] N. Fukuda, K. Sawada, and M. Taketani, Progr. Theor. Phys., Japan, 12 (1954) 156.
- [21] S. Okubo, Progr. Theor. Phys., Japan, 12 (1954) 603.
- [22] V. Bernard, N. Kaiser, and Ulf-G. Meißner, Int. J. Mod. Phys. E4 (1995) 193.
- [23] G. Ecker, M. Mojžiš, Phys. Lett. B365 (1996) 312.
- [24] N. Fettes, Ulf-G. Meißner, S. Steininger, Phys. Lett. B451 (1999) 233.
- [25] N. Fettes, Ulf-G. Meißner, Nucl. Phys. A676 (2000) 311.
- [26] N. Fettes, Ulf-G. Meißner, M. Mojžiš and S. Steininger, Annals Phys. 283 (2000) 273 [Erratum-ibid. 288 (2001) 249].
- [27] A. Krüger, and W. Glöckle, Phys. Rev. C60 (1999) 024004.
- [28] A. Krüger, doctoral thesis, Bochum 2000, unpublished.
- [29] I.S. Gerstein, R. Jackiw, B.W. Lee, and S. Weinberg, Phys. Rev. D3 (1971) 2486.
- [30] V.G.J. Stoks, R.A.M. Klomp, C.P.F. Terheggen and J.J. de Swart, Phys. Rev. C49 (1994) 2950.
- [31] M. Gell-Mann, and F.E. Low, Phys. Rev. 95 (1954) 1300.
- [32] G.F. Chew, Phys. Rev. 94 (1954) 1748.
- [33] G.C. Wick, Rev. Mod. Phys. 27 (1955) 339.
- [34] G. Ecker and M. Mojžiš, Phys. Lett. B410 (1997) 266.
- [35] S. Steininger, Ulf-G. Meißner and N. Fettes, JHEP 9809 (1998) 008.
- [36] J.F. Donoghue, and B.R. Holstein, Phys. Lett. B436 (1998) 331.
- [37] J.F. Donoghue, B.R. Holstein, and B. Borasoy, Phys.Rev. D59 (1999) 036002.
- [38] N. Fettes, V. Bernard, and Ulf-G. Meißner, Nucl. Phys. A669 (2000) 269.
- [39] N. Fettes, doctoral thesis, published in *Berichte des Forschungszentrum Jülich*, No. 3814 (2000); N. Fettes, private communication.
- [40] E. Matsinos, hep-ph/9807395.
- [41] R. Koch, Nucl. Phys. A448 (1986) 707.
- [42] SAID on-line program, R.A. Arndt, R.L. Workman et al., see website <http://gwdac.phys.gwu.edu/>.
- [43] E. Epelbaum, Ulf-G. Meißner, W. Glöckle, and Ch. Elster, Phys.Rev. C65 (2002) 044001.
- [44] S.R. Beane and M.J. Savage, Phys. Lett. B535 (2002) 177.
- [45] S.R. Beane and M.J. Savage, hep-lat/0203003.